2013

Properties of Amorphous Silicon Germanium Films and Devices Prepared Using Chemical Annealing

Zhao Li
Iowa State University

Properties of amorphous silicon germanium films and devices prepared using chemical annealing

by

Zhao Li

A dissertation submitted to the graduate faculty

in partial fulfillment of the requirements for the degree of

DOCTOR OF PHILOSOPHY

Major: Electrical Engineering (Specialization – Microelectronics and Photonics)

Program of Study Committee:
Vikram Dalal, Major Professor
Rana Biswas
Mani Mina
Joseph Shinar
Kristen, Constant

Iowa State University

Ames, Iowa

2013

TABLE OF CONTENTS

Page

LIST OF FIGURES ..... **III**

ACKNOWLEDGEMENTS ..... **IV**

ABSTRACT ..... **V**

CHAPTER 1 INTRODUCTIONS **1**

RESEARCH MOTIVATION 1
FUNDAMENTALS OF SOLAR CELLS 3
PROPERTIES OF A-SI:H AND A-SIGE:H 5
LITERATURE REVIEW 8
SCOPE OF RESEARCH 15

CHAPTER 2 SAMPLE PREPARATION **17**

VHF-PECVD SYSTEM 17
GROWTH CHEMISTRY 18

CHAPTER 3 CHARACTERIZATION **23**

FILM CHARACTERIZATION 23
FILM THICKNESS MEASUREMENT 23
RAMAN SPECTROSCOPY 26
ACTIVATION ENERGY 27
PHOTO AND DARK CONDUCTIVITY 29
FOURIER TRANSFORMS INFRARED SPECTROSCOPY 30
URBACH ENERGY 31
DEVICE CHARACTERIZATION 33
I-V CURVE 33
QUANTUM EFFICIENCY 36
HOLE $\mu\tau$ PRODUCT 38
URBACH ENERGY 40

CHAPTER 4 FILM RESULTS **42**

H2 CA FTIR RESULTS 42
ELECTRICAL DATA 46

CHAPTER 5 DEVICE RESULTS **48**

I-V CURVES 48
QUANTUM EFFICIENCY 50
HOLE MOBILITY-LIFETIME PRODUCT 51
LIGHT SOAKING 54

CHAPTER 6 CONCLUSIONS **57**

REFERENCES **58**

List of Figures

Page
Figure 1 A pn junction solar cell with resistive load 3
Figure 2 Equivalent circuit of a solar cell 4
Figure 3 Device structure of a-Si:H solar cell 5
Figure 4 Electronic density of states in a-Si:H 7
Figure 5 Tauc's gap plotted as a function of
total hydrogen content for chemical annealing a-Si:H 13
Figure 6 FF of the CA solar cell and standard solar cell
as a function of light-soaking time 14
Figure 7 Raman scattering spectra for 3nm-thick a-Si:H film
before and after H2 plasma treatment for 30s 15
Figure 8 VHF-PECVD chamber 17
Figure 9 Schematic diagram of the growth of Si thin films of MGP module 18
Figure 10 The growth process for a-Si:H films 20
Figure 11 Influence of hydrogen on homogenization of the surface 21
Figure 12 Thickness extracted by transmission spectroscopy 24
Figure 13 Tauc energy derived from UV/VIS/NIR spectrum 26
Figure 14 Apparatus for measuring QE using two-beam photocurrent technique 32
Figure 15 I-V Curve of an illuminated p-i-n diode [3] 34
Figure 16 QE spectrum of an a-SiGe:H solar cell 37
Figure 17 QE ratio of a-Si:H solar cells[1] 38
Figure 18 μτ measurement of a-SiGe:H solar cell 40
Figure 19 gives the Urbach energy measurement result of one a-SiGe:H solar cell 41
Figure 20 Gas flow configuration during chemical annealing process 42
Figure 21 Non-CA sample FTIR 43
Figure 22 10 second H2 CA sample FTIR 43
Figure 23 20 second H2 CA sample FTIR 44
Figure 24 30 second H2 CA sample 44
Figure 25 H2 concentration & Si-H to Si-H2 bond ratio 45
Figure 26 Photo Conductivity and Photo/Dark ratio 46
Figure 27 μτ -product of a-SiGe:H film at Eg=1.62eV 47
Figure 28 Typical a-SiGe:H solar cell device structure 48
Figure 29 IV-curve comparison betwen non-CA and CA samples 49
Figure 30 IV-curve of a-SiGe:H sample with 65.5 FF 49
Figure 31 QE comparisons between different samples under zero bias and positive bias 50
Figure 32 QE ratio comparisons among Non-CA, H2-CA, He-CA samples 51
Figure 33 100mT μτ -product comparisons between H2-CA and Non-CA samples 52
Figure 34 20mT μτ-product comparisons
among H2-CA 10sec, H2-CA 20sec and non-CA samples 52
Figure 35 50mT μτ-product comparisons among H2-CA, He-CA and Non-CA samples 53
Figure 36 FF degradation of CA and Non-CA samples 54
Figure 37 QE ratio before and after light soaking of CA samples (10s H2) 55
Figure 38 QE ratio before and after light soaking of non-CA samples 55

ACKNOWLEDGEMENTS

I would like to thank my major professor Dr. Vickram Dalal and my committee members Dr. Biswas, Dr. Constant, Dr. Mina and Dr. Shinar for their guidance and support throughout the course of this research.

In addition, I would also like to thank my friends, colleagues, especially, Keqin Han, Max Noack, Mike Beckman, Jason Jirak, Atul Madhavan, Brian Lewis, Ashutosh Shyam, Emily Evers, Michael Eggleston, the department faculty and staff for making my time at Iowa State University a wonderful experience. I want to also offer my appreciation to those who were willing to participate in my surveys and observations, without whom, this thesis would not have been possible.

Finally, thanks to my family for their encouragement and to my wife for her hours of patience, respect and love.

ABSTRACT

Amorphous silicon germanium solar cells have been extensively used for many years due to the low cost, easy fabrication, tunable bandgap and special properties. However, it is found that the properties of a-SiGe:H materials is not good as a-Si:H, and this limits the application of a-SiGe:H solar cells and brings the stability concern. Recently, it has been shown that this instability is correlated with the presence of multiple bonded Si-H bonds (i.e., SiH_2), and a technique, namely chemical annealing, was suggested to improve the quality and the stability of a-SiGe:H. Although a number of results have been reported to produce good a-SiGe:H films but, no chemical annealed devices with good quality were reported and no systemic study was ever done on it. .

In this work, chemical annealed a-SiGe:H films and devices, and non chemical annealed films and devices were produced in very high frequency plasma enhanced CVD, and systematic experiments were carried out to study the role of chemical annealing in enhancing the quality of a-SiGe:H solar cells.

It is found that the materials were grown using a layer-by-layer approach, where the growth of a thin film was followed by a chemical anneal in hydrogen or helium plasma. Multiple cycles were used to build up the total film thickness. The purpose of the anneal cycle was to subject the material to controlled ion bombardment so as to reduce void density and thereby lead to better microstructure and fewer clustered Si-H and Ge-H bonds. FTIR measurements showed that the films which were prepared using chemical annealing had fewer SiH2 and GeH2 bonds. Electrical measurements showed that the films subjected to chemical anneal had a higher photo/dark conductivity ratio, a smaller Urbach energy and

higher electron mobility-lifetime products. p-i-n and n-i-n devices were prepared on stainless steel substrates. Measurements of quantum efficiency in p-i-n devices showed that the hole mobility-lifetime product was also improved when chemical annealing was used.

CHAPTER 1

INTRODUCTIONS

Research Motivation

Hydrogenated amorphous silicon germanium is widely used for a number of solid state electronic devices, such as solar cells, solid state photosensors, and thin film transistor for liquid crystal displays, photoreceptors, and image pick-up tubes [1]. The extensive applications of a-SiGe:H origin from its several unique features: (1) it has a very high optical absorption coefficient ($>10^5$ cm^{-1}) over the majority of visible spectrum, making extremely thin film device possible; (2) a simple low temperature deposition process is applicable; (3) the tunable bandgap of 1.0~1.7eV lies near the energy at which high solar energy conversion efficiencies are expected; (4) the raw materials is abundant; (5) the materials is easy to dope both p-type and n-type using boron or phosphorous respectively; (6) the electronic properties of electrons and holes are adequate for many device applications.

Although the a-SiGe provides such unique features, one serious problem associated with a-SiGe limits its application.

- The photo-conductivity decreased and dark conductivity increased
- Electron and hole mobility decreased
- Electron mobility lifetime and hole mobility lifetime product decreased
- The Urbach energy increased
- Midgap defect density of states increased

Intensive studies have been carried out to improve the quality of a-SiGe, which includes the development of new deposition techniques and new structures for the devices. Among them, a technique called chemical annealing (CA) process is utilized to improve the quality and stability of a-Si:H. However, this method was never implied on a-SiGe:H deposition before. The fundamental of CA on a-Si:H deposition was describe as below: The instability of a-Si:H is correlated with multi bonded of Si-H such as Si-. CA use ion bombardment to treat deposition surface. It can reorder its structure and then reduce the multi H-bong type, leading to better qualify and stability. The technique consists in growing a thin film, typically 15-30 Å, and then subjecting it to bombardment from plasma, and then repeating the cycle. Both inert and reactive gas ions have been used for the annealing cycle. Although some of results have been reported to improve the stability of a-Si:H films based on chemical annealing technique, no chemical annealed a-SiGe devices with good quality were reported.

In this study, chemical annealing process is utilized to study if it improves the quality and stability of a-SiGe:H solar cells and materials. Systematic experiments will be designed to study the effect of chemical annealing on the properties of the a-SiGe films and solar cell devices.

Fundamentals of Solar Cells

Fig 1 shows the pn junction with a resistive load. Without bias applied, an electric field exists in the depletion region as shown in figure. When photo arrive the, electron-hole pairs can be generated in the depletion region. And then they will be swept out and this produces the photocurrent I_L in the reverse-bias direction as shown.

A voltage drops by photocurrent I_L across the resistant, which forward biases the pn junction. The forward-bias voltage generates a forward bias current I_F. Therefore, the net pn junction current, in the reverse-bias direction is [3]

$$I = I_L - I_F = I_L - I_S[\exp(\frac{qV}{kT}) - 1]$$

where I_s is the ideal reverse saturation current of the pn junction diode. When positive bias applied on the diode, electric field in the depletion region drops due to bias and does not go to zero or change directions.

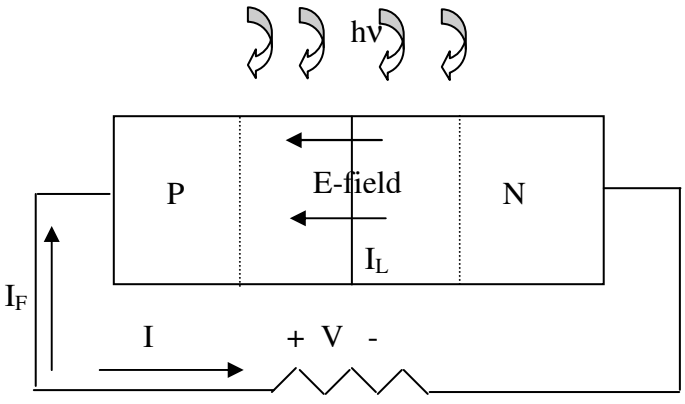

Figure 1 A pn junction solar cell with resistive load [3].

Fig. 2 shows the equivalent circuit of a practical solar cell, where Iph presented photo generated. I_F represents forward-bias current.

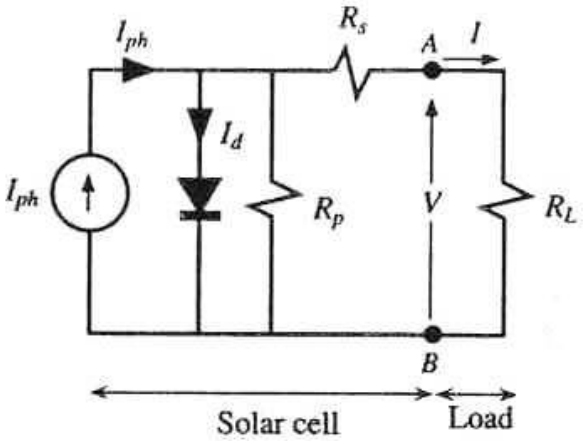

Figure 2 Equivalent circuit of a solar cell [4].

Fig 3 shows the real device structure used in the research. The devices are deposited on rough-polished stainless steel substrates. First, the n layer is deposited using VHF process. The n layer is about 230-250nm thick and it is an a-Si:H layer doped with phosphorus. A thick n layer is needed because of the rough substrate. Next, the i2 layer is deposited, for a-SiGe: H solar cell, using a mixture of hydrogen and silane, or helium and hydrogen, silane, germium. Around 0.3-0.5 of trimethyl B was added to the i2 layer to act as a compensating dopant against the inevitable oxygen contaminant generated during plasma deposition process. The i2 layer is followed by an i1 buffer layer of graded gap a-(Si,C), which can reduce the B diffusion from p layer. It was main reason the thin film solar cell degradation. i1 buffer layer is then followed by a thin (20nm) a-(Si,C) p layer. Finally, an ITO contact is deposited on top.

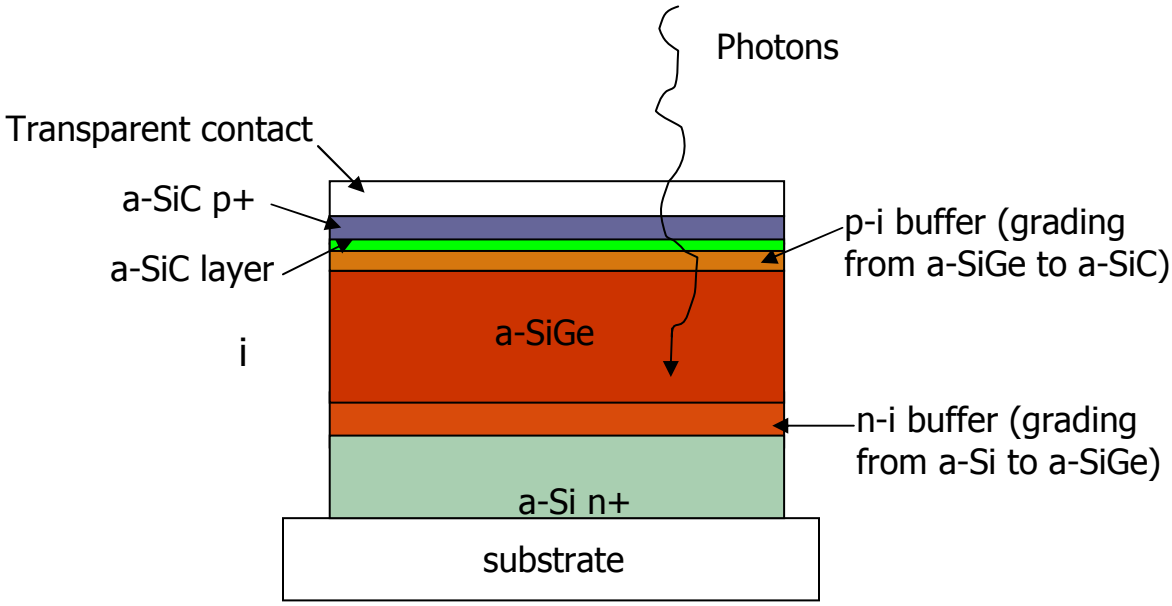

Figure 3 Device structure of a-Si:H solar cell

Properties of a-Si: H and a-SiGe: H

Several deposition techniques, such as plasma-enhanced chemical vapor deposition (PE CVD), hot wire-chemical vapor deposition (hot wire CVD) and reactive sputtering, can be used to produce amorphous silicon germanium. In all these processes, hydrogen is used in the deposition process. Generally, 4-40 atomic percentage of H is in these kinds of films, so we normally name them a-SiGe:H.

Unlike the crystallite structure, we use tetrahedral network model to describe this film atom connection. Here we start with simpler condition with just silicon atoms without any germanium atoms. Atoms with lower co-ordination happen as they locally

release the strain in the disorder structure. It leaves unpaired electrons, also called as dangling bond. These dangling bonds will act as recombination centers and be root cause of solar cell performance degradation. In order to reduce the effect from dangling bonds, hydrogen passivation is used. It was shown in the previous research that the number of dangling bonds is about 10^{20}-10^{22} cm^{-3} in a-Si before being passivated by hydrogen. After the passivation, the number drops to about 10^{15} cm^{-3} [6].

To understand the electronic properties of amorphous structure, it is critical to determine the distribution of the trap states in the bandgap. Fig.4 shows a density of states curve for an undoped a-Si:H film. The lack of long-range order and distortion of the covalent bonds of fourfold co-ordinated neutral silicon atom in amorphous structure gives rise to a gradual, approximately exponential decrease of the density of states, so called band tails, given by

$$N_{TC} = N_{C0} \exp \frac{E_C - E}{E_{urc}}$$

$$N_{TV} = N_{V0} \exp \frac{E - E_V}{E_{urv}}$$

where N_{TC} and N_{TV} are density of states (DOS) for conduction band tail states and valence band tail states respectively; and E_{urv} and E_{urc} are the characteristic widths of the conduction and valence band tails and called the Urbach energy. For a-Si:H, the typical values of $N_{C0} = N_{V0} = 10^{21}$ to 10^{22} $eV^{-1}cm^{-1}$, E_{urv}= 42-45meV and E_{urc}=26meV [7], which means that valence band tail extends deeper into the gap. Low Urbach energy implies less disorder. The optical gap increases from about 1.5eV for pure amorphous silicon, also will vary as Ge atom in added, since a-Ge has smaller bandgap.

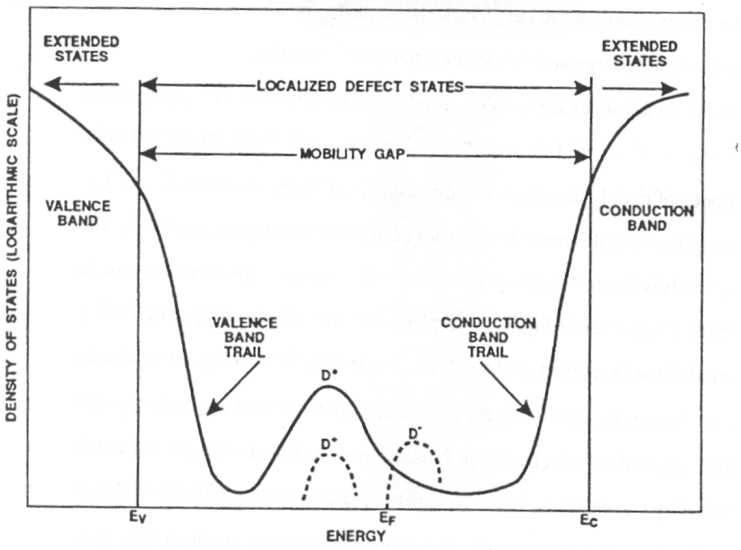

Figure 4 Electronic density of states in a-Si:H [5]

In amorphous silicon or germanium does not hold most of electronics states near bandgap, accordingly, the optical absorption coefficient is much larger than that of crystalline silicon. E_{tauc} is termed the optical energy (or Tauc) gap, and is normally used for defining the energy gap of amorphous semiconductors. The typical value for a-SiGe:H is 1.0-1.7 eV.

$$\alpha = \alpha_0 \exp \frac{h\nu - E_g}{E_{urv}}$$

E_{urv} is called the Urbach energy, which given in above equation. This region can be described in terms of a transition between a band-tail state and an extended band.

Finally, some properties of device-quality a-Si:H, a-SiGe:H is given here:

	a-Si:H	a-SiGe:H
Band Gap	1.7-1.8eV	1.0-1.7eV
Urbach Energy	42-50meV	>45meV
Photoconductivity	10^{-4}s/cm to 10^{-5}s/cm	10^{-5}s/cm-10^{-7}s/cm
photosensivity	10^{5} to10^{6}	10 to 10^{5}
	$>10^{-8}cm^2/v$	$10^{-8}cm^2/v$ to $10^{-10}cm^2/v$

Table 1 Properties comparison between a-Si:H and a-SiGe:H

Literature review

a-(Si,Ge):H has poorer electrical and optical properties than that of a-Si:H. By varying the Ge content in the material, the optical bandgap (Eg) can be modulated from 1.7eV to 1.0eV. When Eg decreases, most research found

- The photo-conductivity decreased and dark conductivity increased
- Electron and hole mobility decreased
- Electron mobility lifetime and hole mobility lifetime product decreased
- The Urbach energy increased
- Midgap defect density of states increased

Let's start with fundamental cause of poor quality from a-Si film. Under the illumination of light exposure, electron-hole pairs will be generated. The photo-generated electron-hole pairs combine in the film and release energy, which breaks weak Si-Si and /or Si-H bonds and creates defects, and in turn deteriorates the conductivity of the film. The degradation process can be described by three models: (1) the Trap-to–dangling bond conversion model, first proposed by Adler and quantified by Dalal [8] proposes that both positively correlated dangling bonds (D^0) and negatively correlated

charged defect states ($T3^-$ and $T3^+$) exist in the a-Si material. The capture of a charged carrier by an oppositely charged defect state leads to the conversion of this trap state into a positively correlated dangling bond state, thereby leading to an increase in D^0 states and an increase in recombination; (2) Bond breaking-SJT model [8], proposes that the energy released by recombination of an electron-hole pair, leading to breaking of weak Si-Si bonds, thereby creating dangling Si bonds which give rise to increased density of midgap defect states; (3) H Collision model [9] proposes that recombination of photogenerated carriers excites mobile H from Si-H bonds, leaving three fold coordinated Si dangling-bond defects. In 1977, Staebler and Wronski found that both the dark and photo-conductivity of a-Si:H, after being illuminated with band-gap light for a long period of time were reduced, with restoration being achieved by annealing at 180^{o}C [2].

Where is a-SiGe, the case become even worse as the following effects:

- The preferential of dissociate GeH_4 rather than to SiH_4
- The preferential attachment of Hydrogen to silicon rather than germanium and the weakness of Ge-H bond, so Ge dangling bonds increases
- More Ge-Ge clustering due to low surface mobility
- More dihydride bonding (buried H), porous structures
- Columnar structure and greater density of voids by inhomogeneous growth of many radicals

Many different approaches have been tried to solve above issues, such as (1) Xixiang Xu et al, Untied Solar Corp.- Rf plasma-enhanced CVD, multi-chamber. By

using Si2H6+GeH4+H2 (Jsc=18.4mA/cm2, Voc=0.73, FF(white)=0.62); (2) Sukti Hazra et al. India Association for the Cultivation of Sci. Rf-plasma enhanced CVD [10]. Using Helium dilution, growth rate 80Å/min(1.3A/sec) has been achieved with defect density=6.72E15cm-3eV-1 and Urbach energy=46±1.5 meV. (3) Xixiang Xu et al, United Solar Systems Corp. RF-PECVD. H2 dilution effect was studied; high H2 dilution increases the performance. Si2H6-GeH4-H2, thickness for intrinsic layer is ~4000Å with Jsc=18mA/cm2, Voc=0.74, FF(white)=0.59. (4) Sanyo's group using VHF-PECVD ~ 70MHz, 150mT, 230C. They use hydrogen dilution ratio 25~54 to achieve deposition rate 1.4A/s with hydrogen content ~10%, Si-H/Si-H2<4 but No-systemic hole mobility-lifetime product were reported (5) United Solar using lower Temperature filament ~1750C which help to get hydrogen Content 12.3% for about 10% GeH4 in the feed gas. The cell can be Voc=0.625 V, Jsc=20.91 (mA/cm2), FF=53.6%, η=7% (6) D.Lundszien et al, Institute of Photovoltaics, Germany. They check the effect of a-Si:H buffer layers (pi/ni) in a-SiGe:H solar cells and discussed the effects of buffer layers' profile, thickness, bandgap, and position. The best solar cell can reach Jsc=6.4mA/cm2, Voc=0.685eV, FF(AM 1.5 and a 590 nm cut on filter)=0.69, Eg=1.5eV.

Meanwhile, light-induced degradation of a-Si:H is shown to be related with hydrogen concentration, especially with Si-H_2 (C_{SiH2}) bond density [11]. According to the growth chemistry of a-Si proposed by Dalal [13], this can be explained by the microvoids introduced by the extra H or SiH2. If the surface hydrogen is not removed and Si not cross-linked, the bonded Si-H structure gets buried, new material grows

around it, and a microvoid forms once the Si-H bond breaks down. The shift in IR signal can arise from H bonded at internal surfaces of voids. The SiH2 radical introduces the same problem (mirovoid) like extra H does. By combing the SAXS results with infrared measurements, Williamson et al [14] deduced that at the interior surfaces of these microvoids are largely un-hydrogenated after degradation, containing at most 4-9 bonded H atoms. Moreover, the presence of microvoids also allows the existence of the SiH2 polymer chains in the material. These chains are a primary cause of the degradation, since H there is loosely bonded, compared to the random Si-H bond in the bulk, and breaks rather easily upon energetic excitation [15]. The detailed discussion will be provided in the section growth chemistry.

In order to eliminate the extra H and get a structure with fewer voids, there are two ways to achieve such goal.

(1) Using high temperature of growth. A higher deposition temperature will break the weak Si-H and thus provide more energy Ge atom to remove right location. However, increasing temperature of growth may result in the breaking of some inevitable weak Si-Si or Si-H bonds, thereby introducing defects.

(2) Using ion bombardment. We can use both reactive species like H, and non-reactive ion like He. The role of both ion bombardment can be describe as

- H ion

  - reactive, can take away the H bond by reaction

  - breaking the bonded H by impinging

  - can penetrate into the subsurface

- He ion

  - not reactive

  - heavier ion bombardment

  - breaking surface bond, creating dangling bonds

  - provide momentum for SiH3, GeH3 radicals

The process of eliminating the H also can be treated as the process to eliminate the SiH_2 bond. Si-H_2 radical is considered to be originated from the contribution of higher-order-silane related radicals like Si_2H_6, SiH_8…, which forms internal voids. Low pressure and high H dilution prevent formation of these higher radicals. [1]

Recent years, a new technique called "chemical annealing (CA)" or "layer by layer deposition" is introduced to remove the H. During each cycle, the first is deposit 15-30A film and followed by H, Ar, He ion bombardment. Through many of these cycles, certain thickness of amorphous film thickness could be achieved. In addition to this process, some researchers applied an alternative process, in which the deposition is composed of periodic low hydrogen dilution layer and high hydrogen dilution layer [33, 34].

The advantage of CA process is each growth layer is followed by an immediate ion bombardment; it can ultimately improve the efficiency of ion bombardment, as each atom will have certain penetration depth.

The fundamental work is first represented by the Shimizu group [35-39]. The important results from Shimizu's group can be generalized as:

(1) Optical band gap (Tauc gap) of a-Si:H was varied from 1.5eV-2.0eV. By varying deposition time(t1)/H ion treatment time(t2) as well as substrate temperature and RF power

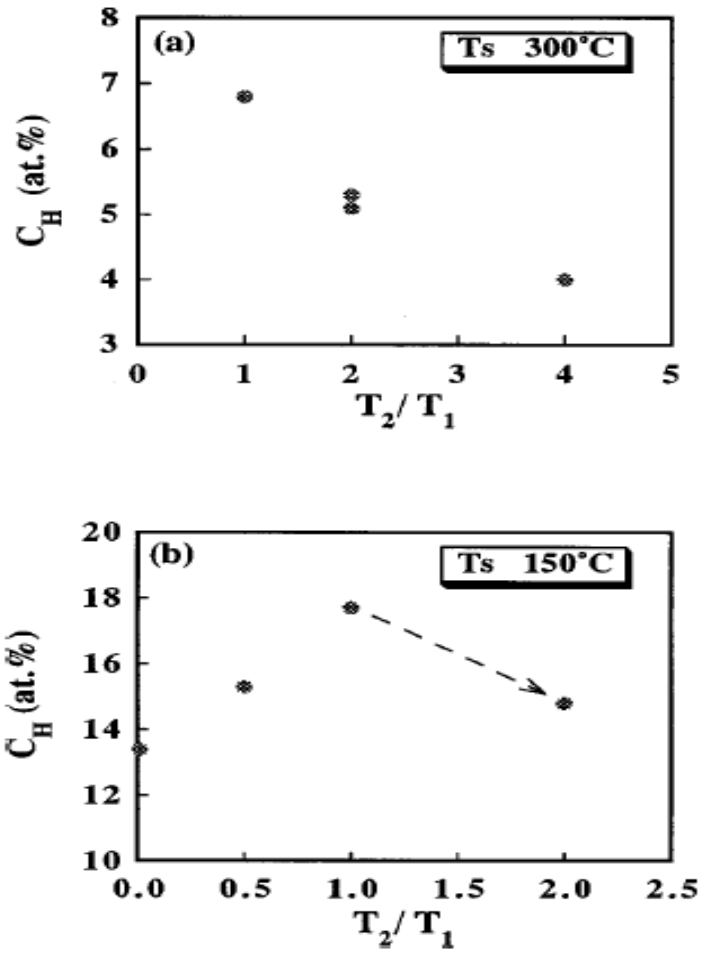

Figure 5 Tauc's gap plotted as a function of total hydrogen content for chemical annealing a-Si:H [16]

(2) Ar radical or ion treatment is applied as well, makes the band gap smaller, Ar ion bombardment breaks the Si-H and decrease the H content, This in turn decrease the bandgap of a-Si:H. Measurements showed that a varied bandgap from 1.62eV to 1.52eV can be obtained.

(3) When substrate temperature is higher than 200°C, hydrogen radical flux was found to promote crystallization. While when the addition of Ar ion is introduced into H, the crystallization was partly prevented with the aid of ion-bombardment [18]

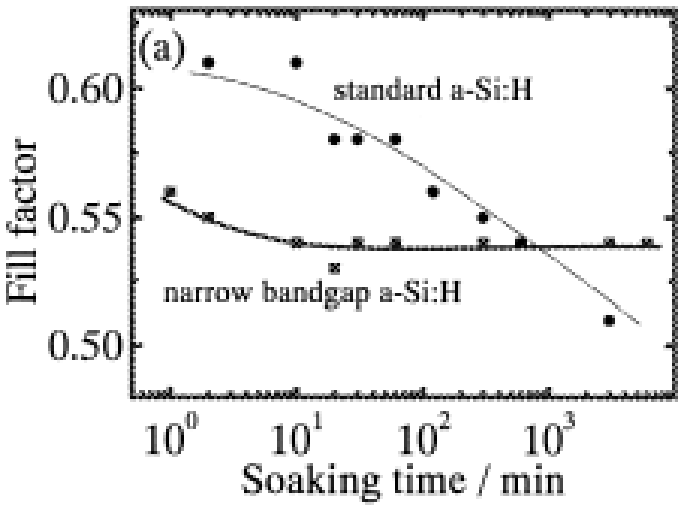

Figure 6 FF of the CA solar cell and standard solar cell as a function of light-soaking time [17].

(4) p-i-n solar cell is built by Ar CA. The original FF is ~ 57% **POOR** Stability is compared with standard a-Si: H solar cell. After a light soaking of ~700 minutes, the FF of the standard one drop below that of the CA one (shows as above)

The most coinciding demonstration that CA by H plasma significantly improves the microstructure of a-Si was provided by work in Prof. Hirose's group [19]. In Figure 7, Raman scattering spectra for a 3 nm-thick a-Si:H film shown that the band intensity due to the wagging mode of SiH_x decreased after the H_2 plasma treatment while the

intensity due to the a-Si TO-like phonon increased, which indicates the hydrogen desorption from the hydrogen-rich surface layer during the H_2 plasma treatment.[1]

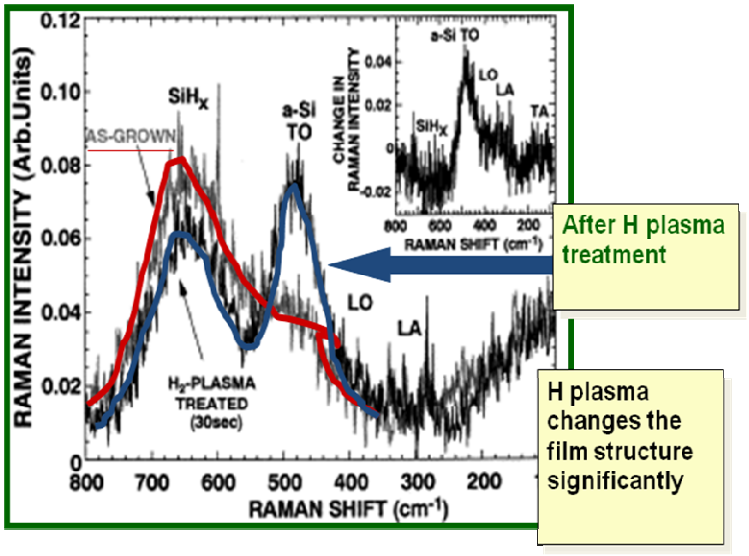

Figure 7 Raman scattering spectra for 3nm-thick a-Si:H film before and after H2 plasma treatment for 30s [19].

Scope of research

A-Si cell has been studied by Shimizu group [16-20]. Besides, application on a-SiGe:H was not applied but also some fundamental questions are still not solved.

(1) He and Ne have been used for CA process as well. Narrow band gap (<1.6eV) A $\mu\tau$ product of 7×10^{-8} cm^2/V for electrons and 3×10^{-8} cm^2/V for holes were claimed [19]. But this value for hole $\mu\tau$ product does not agree with poor FF, and electron $\mu\tau$ product too low by 10x

(2) Although the CA provides improved stability for p-i -n devices, the FF are very poor (<55%).

In this research, systematic experiments will be designed to study the chemical annealing technique, and see if it can improve the quality and stability of a-SiGe:H solar cells and materials.

(1) Chemical annealed a-SiGe:H films prepared by H (plus He) plasma will be made. Previous studies in our group show the necessity for having both H and He or Ar present to prepare good films [21]. In the meantime, the non-chemical annealed a-SiGe:H films prepared by He (plus H) will be prepared. The comparisons between CA films and non CA films will be studied. This includes H concentration, hole mobility, the SiH_2 bond density, the optical band gap and the stability of films in photoconductivity and etc.

(2) Systematic study of devices will be carried out as well. A more stable CA device with good FF is the goal. Both the He (plus H) and H plasmas will be applied.

(3) The stability between CA devices and non-CA devices will be compared. Fundamental electronic properties of the CA and non CA devices, which includes the holes' $\mu\tau$ product, QE, QE ratio, will be studied before and after light soaking.

CHAPTER 2

SAMPLE PREPARATION

VHF-PECVD system

The deposition system used in the research is very high frequency plasma enhanced chemical vapour deposition system (VHF-PECVD). The frequency of the microwave energy source is 45MHz. Through a power gain generator a couple of watts power was feed into capacitor couple plasma system. The feed-stock gas is introduced to the deposition chamber directly, which means that the gas will be decomposed in the same chamber as deposition.

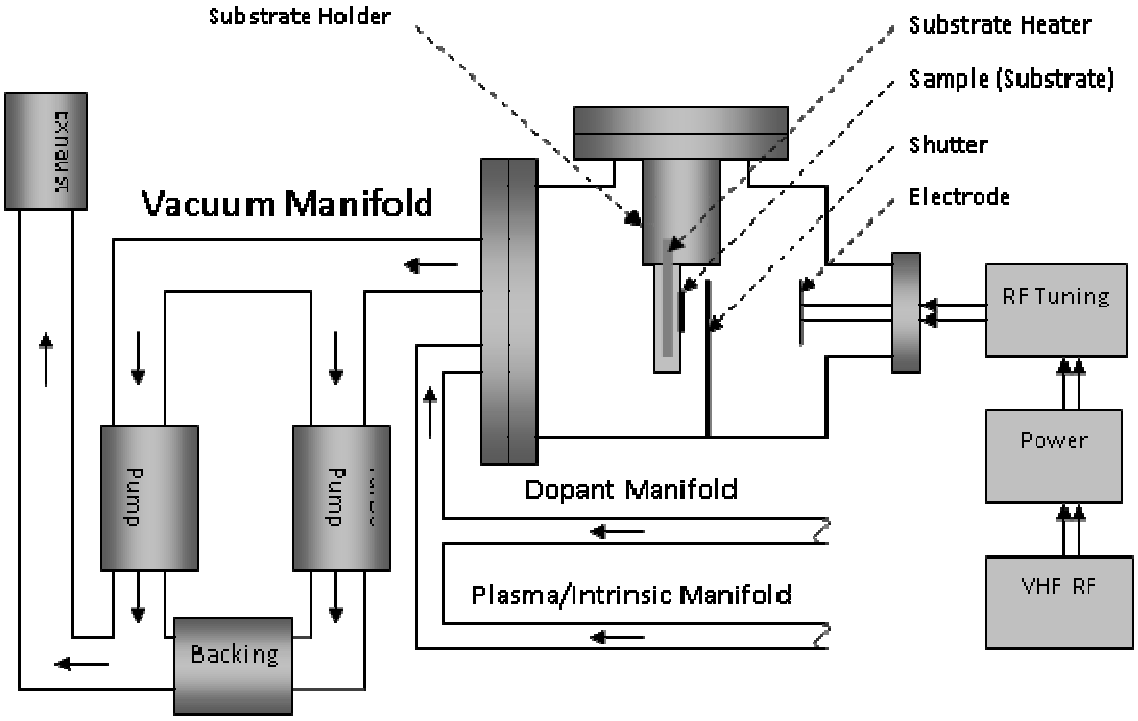

Figure 8 VHF-PECVD chamber

Growth Chemistry

As a-SiGe growth is very similar to a-Si, here we use a-Si:H growth model to describe first. The standard model of a-Si:H growth is called MGP model. According to Matsuda [22], Perrin [23] and Gallagher [24], it states that the growth of a-Si:H is limited primarily by surface diffusion of a radical such SiH_3. When this radical finds an open site, it bonds, and H is eliminated by breaking of Si-H bonds and subsequent cross-linking of neighboring hydrogen boned to adjacent Si atoms. The schematic diagram of the MGP model is shown in Fig. 9. However, a silyl radical bonded to a surface Si is relatively stable; and the bond breaking energy is ~2.5 eV. Therefore, other mechanism or energy is needed to remove this H. With this model, we cannot simply explain how H ion could be removed by chemical process or ion bombardment.

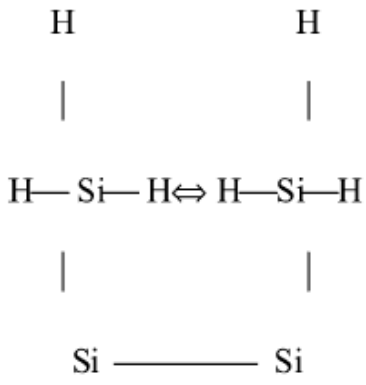

Figure 9 Schematic diagram of the growth of Si thin films of MGP module

Later Dalal' module suggested that the primary consideration which determines the growth of high quality a-Si:H and alloy films are the removal of surface hydrogen.

This removal is not by reaction between adjacent bonded H, but by extraction of another H radical. A high H dilution leads to a significant concentration of H ions and radicals impinging on the surface, and these remove bonded H [13]. The H ions are able to penetrate 15-30A deep into film, and remove some more bulk H underneath. The role of inert gas ions, such as Ar and He are only to break the surface H bonds, which either creating a dangling bond or allowing another silyl radical to insert itself. As mentioned in last chapter, the inert gas ions do not penetrate deep into the substrate, but H ions do.

According to Dalal's model [25], the growth of a-Si:H is not a simple process. In particular, at least 3 separate steps appear to be necessary for growing good a-Si:H. These steps are: (1) Removal of surface H; (2) Insertion of a SiH_3 radical into the open bond; (3) Removal of inter-atomic H and cross-linking of Si. The whole process is shown in Fig. 10. [1]

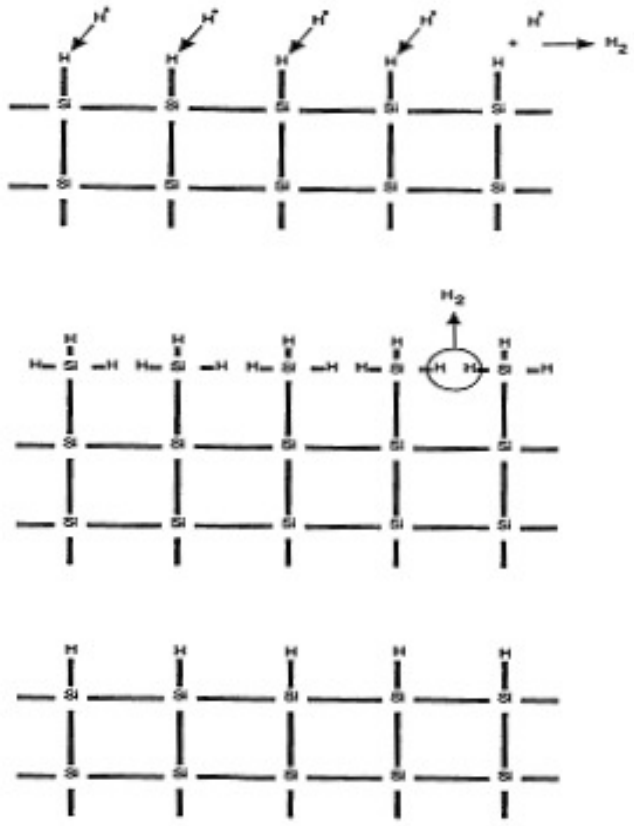

Figure 10 the growth process for a-Si:H films [26]

If the surface hydrogen is not removed and Si not cross-linked, the bonded Si-H structure gets buried, new material grows around it, and a microstructure with a significant void concentration and clustered silicon-hydrogen bonds form in the lattice. As shown in Fig. 11 [26], since both SiH_2 and SiH_3 are present in the radicals flux, they both insert in a Si dangling bond at the surface [1]. After insertion, bonds with H are passive but the one with dangling are. However, when significant excess of H radicals is present, H homogenizes the growing surface by first attaching itself to the surface dangling bond, then the next H atoms serves to remove the bonded H, and create an

active site [26]. And this is true for all the sites; irrespective of which radical (SiH_2 or SH_3) was bonded at the site. Thus, the presence of H serves to homogenize the surface [1].

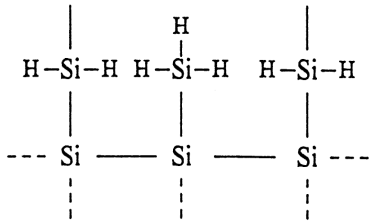

A non-homogeneous surface
in the absence of H dilution

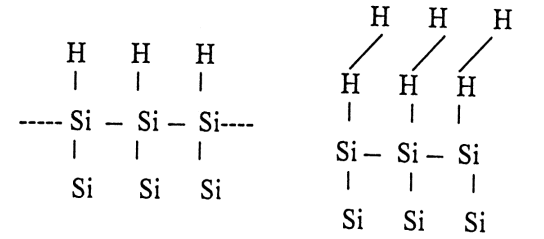

A. Homogenization of surface by H

B. Hydrogen extraction

Figure 11 Influence of hydrogen on homogenization of the surface [26]

The mechanism of SiH_2 on the growth of a-Si:H can be shown in above figure. For a homogeneous surface, first H removes the surface H and leaves open sites, then SiH_3 radicals insert to the open sites, then the adjacent Si-H is broken by other forces such as ion or thermal energy and atomic H combines, and then cross-linking of Si takes place. Therefore a homogenous surface can be formed and surface dangling bond are passive by H. For continuous growth, the dangling bond can be broken by the force mentioned in above and then can accept other radicals. However, if the extra H is not extracted before new radical arrive, it will be buried by the material growing around it.

And a microstructure with a significant void concentration and clustered silicon-hydrogen bonds could form in the lattice This Extra H brought into film during deposition results in microvoids, which leads to the light-induced degradation. The interior surfaces of these microvoids may be unhydrogenated.

Based upon above model, chemical annealing process help to remove access H on the surface of Si film and also provide addition energy for Ge atom for mobility. Typically 15-30 Å film growth and then subject it to bombardment from plasma, and then repeating the cycle. During the ion treatment period, the highly energetic ions are supposed to break the weak Si-H bonds and take the excess H away by combining them with the H ions. And this reduces the micro-voids induced by the excess H and improves the quality and the stability of a-SiGe:H in the future application.

CHAPTER 3

CHARACTERIZATION

Film characterization

Film thickness measurement

A full spectrum spectrophotometer is used to determine the film thickness and the optical band gap from the absorption coefficient variations with photon energy. Through split-beam, spectrophotometers generate twp parallel beam from same power light source. One of them is direct to photo-detector and another is shine on the sample surface. Then the spectrophotometer compares the transmissions difference collected from photodetector on both beam.

Assumption is that the light not transmitted through the sample and collected is either reflected or absorbed. A typical example of transmission vs. wavelength spectra is as shown in figure 3.1. The thickness of the film can be calculated from below equation: [28]

$$t = \frac{(\lambda_1 \lambda_2).m}{(\lambda_1 - \lambda_2).n}$$

m=1/2 for peak to peak and 1/4 for peak to valley (Fig. 12) and n is the refractive index of the material. The refractive index varies with wavelength and can be calculated from the average value of reflection. With assumption of constant deposition rate, growth rate can be calculated out with knowing deposition time.

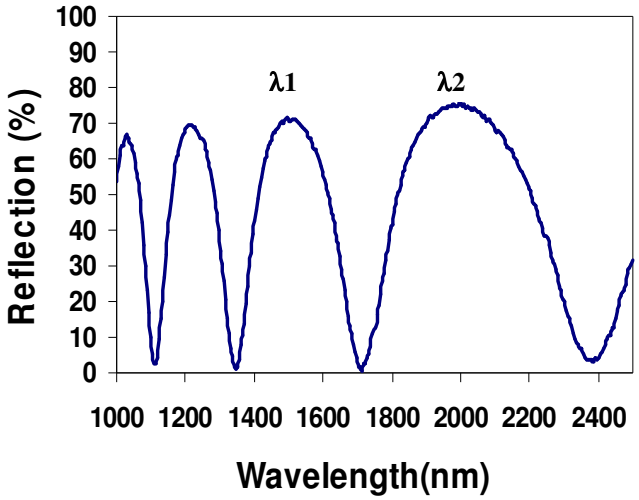

Figure 12 Thickness extracted by transmission spectroscopy [1]

Beside the film thickness, the absorption coefficient can also be obtained. We can use the following expression to calculate the absorption coefficient as a function of wavelength

$$T(\lambda) \approx (1-R)e^{-\alpha(\lambda)t}$$

$$A(\lambda) = \log_{10}\frac{I_i}{I_t} = \log_{10}\frac{1}{T(\lambda)}$$

where A(λ) is known as optical density, T(λ) is the transmission and t is the thickness of the film, and α(λ) is the absorption coefficient. Then the absorption coefficient can be given as

$$\alpha(\lambda) = \frac{\ln(1-R(\lambda)) + 2.303A(\lambda)}{t}$$

And then we can estimate the band gap based upon the absorption coefficient at center wavelength. The optical gap can be approximated as the energy where the absorption coefficient is equal to10^4 cm^{-1}, known as the E04 energy.

Another way to evaluate the band gaps is also known as Tauc's, shown in below equation. It also describes the absorption that occurs at photon energies above the E04 energy. It is easy to find out the intercept of line $(\alpha\hbar\omega)^{1/2}$ vs. photo energy will be Tauc' band gap.

$$\alpha\hbar\omega = B(\hbar\omega - E_{Tauc})^2$$

For a certain film, above two method results should agree with each other and the rule is normally that E_{tauc} is ~0.15 eV less than E04 for hydrogenated amorphous silicon or silicon germanium. A typical plot used for the determination of Tauc's gap is shown in Fig. 13. It is more accurate to obtain the Tauc's gap by determining the slope of the linear region although a lot time it may be very difficult.

Since we are study amorphous materials, it will be very importance to measure these bandgaps. As we know, significant difference between amorphous material and crystal material is bandgap. The measurement will give us clear signal of degree of crystallinity of certain material. However, this tests for crystallinity maybe ambiguous, later we will introduce Raman as more accurate measurement method. But information obtained here will be good indicator of first order.

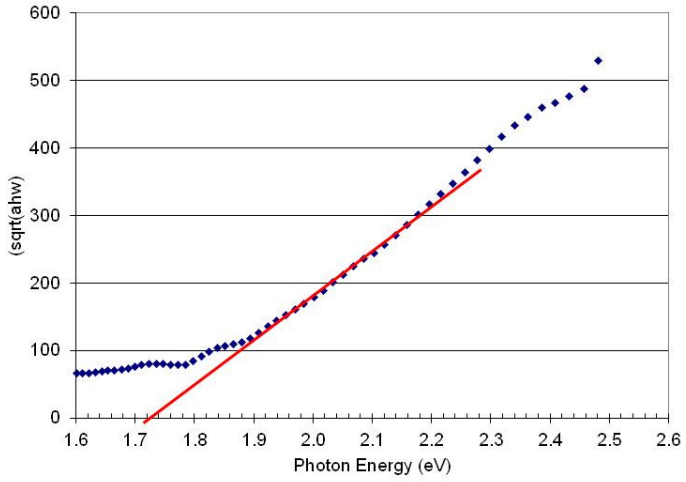

Figure 13 Tauc energy derived from UV/VIS/NIR spectrum

Raman Spectroscopy

Raman spectroscopy here is this research is used to obtain the degree of crystalline quality of the films and determine whether the film is in amorphous phase or crystalline phase. Normally a laser beam is used in this technique. Scattered light from the sample is collected by light detector right on top of samples. Most of the scattered lights hold same frequency as the incident laser beam. Other scattering light which has information lattice vibration is what we need to measure. Based upon the energy and momentum conservation equations shown in below where the subscripts s, i, and p refer to scattered, incident, and phonon, respectively.

$$\hbar\omega_s = \hbar\omega_i \pm \hbar\omega_p$$

$$\hbar k_s = \hbar k_i \pm \hbar q_p$$

Here is the minus sign refers to Stokes scattering and plus sign refer to anti-Stoles scattering. As photon momentum is very small, the photo produced from Raman scattering will be limited to the center of the Brillouin zone. With momentum conservation, crystalline silicon, amorphous silicon and amorphous germanium hold unique peak for identification. For crystalline silicon, there is only one active phonon mode at 520cm^{-1} [29]. Amorphous silicon, on the other hand due to its lattice formation, can have a variety of phonon modes, with the most intense peak around 500cm^{-1}. Therefore by comparing the position and shape of the Raman peaks we can determine whether the material is crystalline, amorphous.

Besides, peak width defined by full width at half maximum (FWHM) indicates the crystalline quality of the material. For amorphous materials, disordered lattice give relaxation to the momentum conservation limitation on the phonon mode occurs. Therefore, the Raman peak collected will become wider. By looking at the change in peak width of a film with respect to the germanium wafer, the crystalline quality of the film can be evaluated.[1]

Activation Energy

The activation energy is one key parameter to determine the conductivity of intrinsic films. As below equation shown, the conductivity of a semiconductor film is proportional to the number of carriers available in the film. Where E_A is activation

energy, k is Boltzman's constant, T is the temperature in Kelvin, and σ_0 the baseline conductivity, or pre-exponential factor.

$$\sigma = \sigma_0 e^{\frac{-E_A}{kT}}$$

As the intrinsic concentration of carriers is dependent upon temperature, conductivity will vary with the material temperature according to an Arrhenius relationship. Using above equation, we can easily obtain the activation from plot of natural logarithm of measured conductivity versus sample temperature. For amorphous, such as a-SiGe:H, which normally is lightly doped semiconductors, the most of electrons will be located in states at or below the Fermi energy. As these carriers are needed to be energized into the conduction band for current to flow, E_A become the measurement of the location of the Fermi energy in amorphous materials.

During the measurement, we use heat pad to heat the samples to 210°C with 100V vias applied cross aluminum bar deposited on the film. Then we take current measurement from 210°C to 130°C with 10 degree interval and then plot natural logarithm of current versus 1/T. The linear regression gives the slope of K times E_A. So we can determine the activation energy.

Photo and Dark Conductivity

For solar material, the conductivity under light is essential. However, the conductivity under dark condition will also tell us film quality and defect states in the film. We need to examine both conditions to understand the quality of the film. This ratio of above conductivities is known as the photosensitivity of the material and is a general indication to the quality of the material as high quality a-Si:H has a photosensitivity greater than 105, a-(Si,Ge):H with an E04 gap of 1.5 eV is ~102, and doped crystalline silicon or germanium should be ~1.

This measurement is performance in the instrument consisting of a large aluminum heat sink cooled by a fan placed in a light impervious box. We measure current between two precise deposit contact bars on film surface, with 100v bias applied. Steel panels and an aluminum door sealed with Velcro and magnets enclose the sample and heat sink to form the light-tight box which can block all light during the dark conductivity measurement. And normally, the sample needs to have more than 10mins stabilization time before all early photon generated carrier combined. The photo current is measured while a lamp with AM1.5 (100mW/m2) on top of samples and has a calibrated aperture between itself and the samples in order to maintain AM 1.5 condition.

Then we can use the following equation to calculate conductivity for both conditions, where width between the coplanar contacts is W, the current measured is I. Here in our test the ratio of L/W is 20.

$$\sigma_{L,D} = \frac{WI}{LVt}$$

Fourier transforms infrared spectroscopy

Fourier-transform infrared spectroscopy is able to detect the composition, the microstructure, and the content of materials. We use is here to determine the H content and H bonding states. The infrared range from 5 to 50 μm is incident on our a-SiGe:H samples. A lot of photon will be absorbed by band feature, free charge carriers, or impurities. In the mid-infrared region, the interaction with the sample results in rotational and vibration transitions of the molecules. The wavelengths of the absorption peaks correspond to specific chemical bond and mass of atoms, which can help us determine the H-bond state. The spectral distribution of the absorption peaks of various silicon-hydrogen boning modes has been identified by Brodsky et al [30] and can be roughly categorized into three modes: (1) the Ge-H stretching mode (1890 cm^{-1}) (2) the Si-H and Si-H_2 stretching mode (2000-2100cm^{-1}), (3) the SiH_2 and SiH_3 bond bending scissors mode (840-890cm^{-1}). In our test, no strong Ge-H2 stretching mode is noticed.

We use the method proposed by Brodsky, Cardona and Cuomo (BCC) [31] to calculate the H concentration. Double-side polished Si wafers were used as substrate for this study, as it can prevent diffuse reflection from the backside of the substrate. The following equation gives the hydrogen content in a-Si:H [32]:

$$N_H = A\int \frac{\alpha(\omega)}{\omega} d\omega$$

where A is an experimentally determined constant and for wagging mode is 1.6×10^{19} (cm^{-1}), $\alpha(\omega)$ is the absorption coefficient at angular frequency ω. The integral extends over the whole $640cm^{-1}$ absorption peak.

Urbach energy

Urbach energy of valence band tails and mid-gap defect densities are important parameters for determining the performance of amorphous film and also devices. In particular, the tail states limit the movement of level upon light excitation, and thereby provide a limit or potentially reduce open-circuit voltage which can be developed in an a-SiGe:H solar cell. The mid-gap states are effective recombination centers for excess carriers, which limit the minority carrier's diffusion length. Therefore, Urbach energy is a good measure of amorphous material quality.

A good quality a-SiGe:H material should have low Urbach energy which normally around 47-50meV. The traditional way to measure Urbach energy of films is based on sub-gap photoconductivity techniques, which rely on optical excitation from these states, into conduction band and then measuring photoconductivity of the material versus wavelength of light.

The dual-beam photoconductivity technique developed by Wronski et al. [33], where a strong DC beam is used to fix the quasi-Fermi levels of the material, by keeping available states in the mid-gap region filled with photo-generated carriers. At same time, a second beam with 13.5 Hz controlled by a chopper to remove noise associated with the

60 Hz current used to power the equipment. The 2nd beam supply additional carriers and increase the conductivity. We measure the film conductivity change with same frequency of chopper, and filter out other noise. The wavelengths used for typical a-SiGe:H characterization varies from 1200 nm to 600 nm, and filters with roll-off frequencies of 700 nm, 900 nm, and 1200 nm are used. A schematic of the device used in the dual-beam photoconductivity technique is shown as Fig. 14.

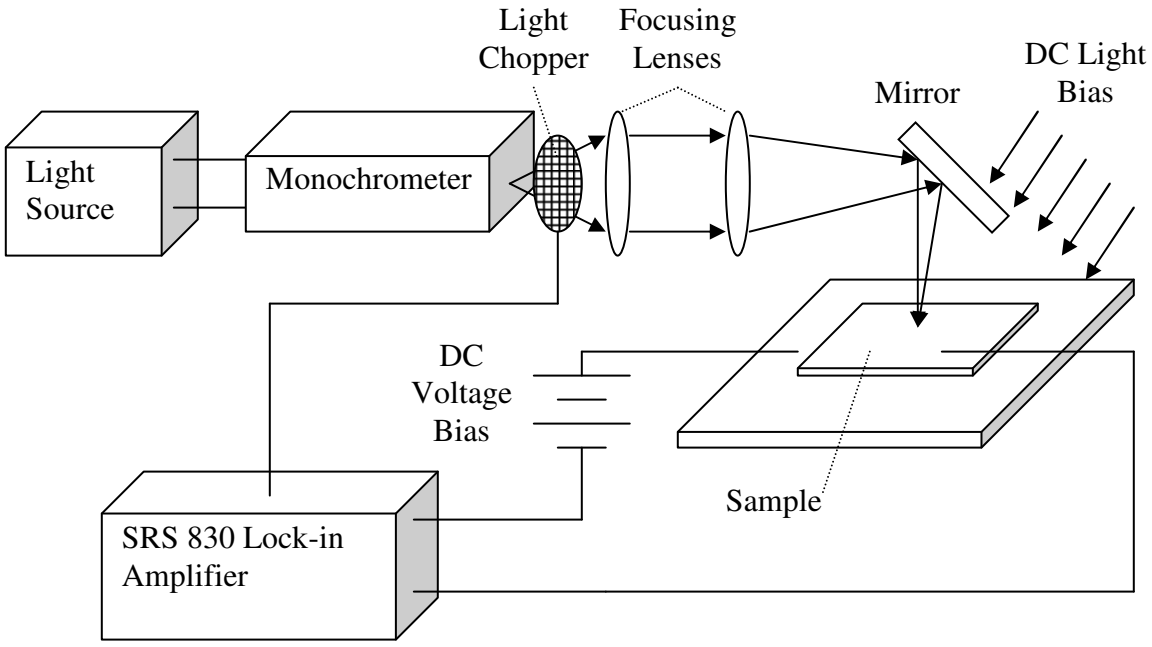

Figure 14 Apparatus for measuring QE using two-beam photocurrent technique

The 2nd light beam is collimated through lenses and focused onto the sample by a mirror. We measure the additional current generated by this light beam using lock-in amplifier to determine absorption coefficient. Using below equation, E_{ur} can be determined with above absorption coefficient with photon wavelength and band gap.

The inverse slop of the natural logarithm of absorption coefficient α versus photon energy gives us the Urbach energy.

$$\alpha = \alpha_0 \exp \frac{h\nu - E_g}{E_{ur}}$$

where E_g is the band-gap, *h* is Planck's constant and ν the wavelength.

Device Characterization

I-V Curve

The key performance of a solar cell under light source normally is characterized by current voltage dependence. A typical current-voltage curve (I-V) of a p-i-n solar cell under illumination is shown in Fig 15. From the equivalent circuit, we use three parameters to grasp the complete description of the electrical behavior of solar cell.

The current-voltage relationship is described in the following equation:

$$J(V) = J_s[e^{\frac{qV}{AkT}} - 1] - J_L(V)$$

where J(V) is the current J at voltage V, J_s is the reverse saturation current, q is the electronic charge, A is the diode factor, K is Boltzman's constant, T is the temperature and J_L is the light generated current.

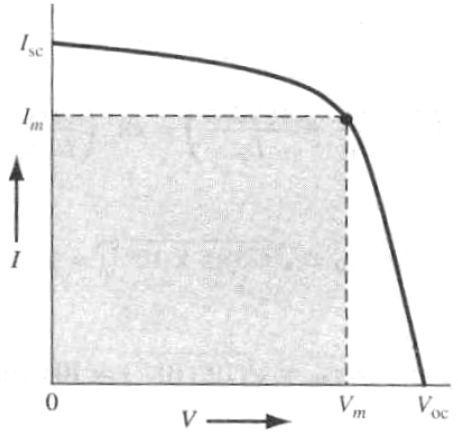

Figure 15 I-V Curve of an illuminated p-i-n diode [3]

In above chart short circuit current J_{sc} or I_{sc}, which is the current of the cell under illumination when V=0. Normally high short circuit current needs good material quality and optimized design of solar cell. J_L in above equation, the photo-generated current, or the short-circuit current, depends on the materials response to the incident and solar cell's collection efficiency, which normally described as:

$$J_L = q\int (1-R)Q(E)S(E)dE$$

where R is the reflection coefficient, S(E) is the spectrum of the light source and Q(E) is the collection efficiency of the solar cell.

Another important parameter from the graph is the open-circuit voltage V_{oc}, which is obtained for J(V)=0. Generally, Voc can be expressed as

$$V_{oc} = \frac{AKT}{q}\ln(\frac{J_L}{J_s}+1)$$

For a diode junction dominated by depletion, the saturation current can be defined as [34]

$$J_s \approx \frac{qn_i W_d}{2\tau}$$

where $n_i = \sqrt{N_C N_V}\exp(\frac{-E_g}{2KT})$,

Therefore, Voc can be described as:

$$V_{oc} \approx \frac{KT}{q}\ln(\frac{J_L}{J_s}) \approx \frac{KT}{q}[\ln(J_L) - \ln(\frac{qW_d}{2\tau}\sqrt{N_C N_V})] + \frac{E_g}{2q}$$

where E_g is the band gap, n_i is the intrinsic carrier density, W_d is the depletion width of the p-i-n junction.

The last but very important parameter from I-V curve is fill factor (FF), which is The maximum possible power solar cell can output at certain illumination condition. Fill factor is given by the ratio between the real optimum output power P_{max} ($=I_m \times V_m$) and the ideal optimum output power P ($=I_{sc} \times V_{oc}$), so it can be described as:

$$FF = \frac{V_m I_m}{I_{sc} V_{oc}}$$

Based on Voc, Isc, and FF, the energy-conversion efficiency η of the solar cell can be calculated. The energy conversation efficiency is the ratio of maximum power that a solar cell can generate under given illumination conditions:

$$\eta = \frac{FF.V_{oc}.I_{sc}}{P_{in}}$$

where P_{in} is the equivalent total incident power of the light photons.

Quantum efficiency

Quantum efficiency (QE) is defined as the ratio of the number of charge collected to the number of incident photons on the sample at a particular wavelength. For typical p-i-n solar cell, QE is defined as

$$QE\ (\lambda, V) = \int_0^t \alpha(\lambda).e^{-\alpha x}.e^{-\int_0^x \frac{1}{\mu\tau\varepsilon(y)}dy}.dx$$

where α is the absorption coefficient, a function of photon wavelength λ; μ is the carrier mobility, and τ is the carrier lifetime, t is the thickness of intrinsic layer, and ε (y) is the electric field.

We use similar tools setup shown in Fig 3.4 to measure QE. However, the difference is that for device, we normally use wavelength range from 400nm to 800nm with the interval of 20nm. This wavelength range cover major output portion from typical solar cell, however, for some smaller bandgap a-SiGe:H cell, we even take wavelength up to 1000nm. The forward and reverse bias voltages can be applied to the cell to simulate operation conditions and to enhance or reduce the internal electric field.

A lot of information can abstract from QE measurement on solar cell. It can help us understand film quality and solar cell design structure. (1) The thickness of the p+ layer can be evaluated by QE values at short wavelengths (400nm). Too thick a p+ layer would lead to a very low QE value and too thin a p+ layer would result in unreasonably high QE. (2) QE values at long wavelengths (~700nm) tell the effect from material quality of intrinsic layers, but also the refection from texture substrate. (3) The position

of the maximum QE in the spectrum can give first order estimation of the thickness of intrinsic layer. When the thickness of i-layer is reduced, the maximum QE position will shifts towards shorter wavelengths. A typical a-SiGe:H solar cell is as below:

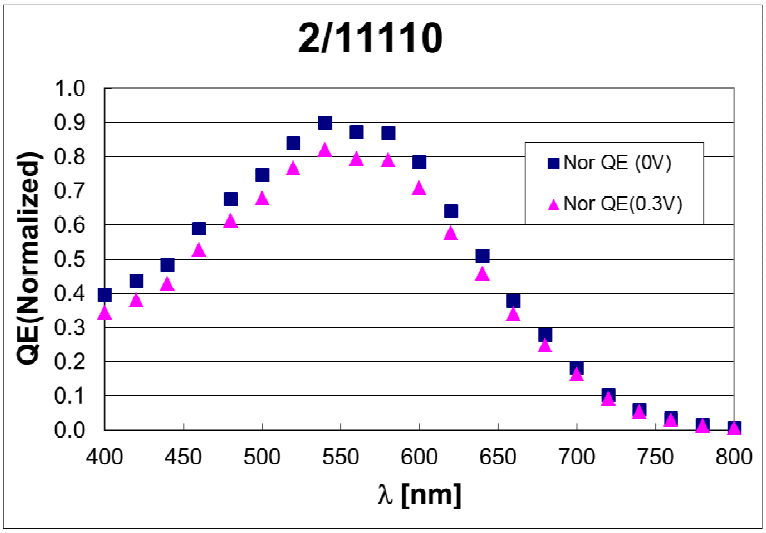

Figure 16 QE spectrum of an a-SiGe:H solar cell

QE measured under bias can tell us about the electric filed profile inside the solar cell [1]. When the solar cell is under forward bias, the internal electric field is reduced by external bias. The carrier collection efficiency can be reduced as the carrier collection of a-SiGe:H solar cell relies on the assistance of the internal electric field due to low $\mu\tau$ products comparing to crystalline solar cell. For a high quality solar cell, the internal electric field is so strong that a small forward bias (such as 0.3v) applied to the cell will not affect the carrier collection efficiency to a great extent.

The ratio of the QE values between zero bias and positive bias can provide us how well the device absorbs and collects the photons of various wavelengths through various locations in the cell. Normally lower energy photons are absorbed further deep

from top p-layer, but high energy photon are absorbed on top layer close or within p-layer. Therefore, the holes generated at deep intrinsic layer have travel all the way through i-layer to be collected. Thus, high QE ratios at long wavelength indicate the holes were generated but no collected. Low QE ratio indicates that the quality of intrinsic material is high enough to collect the holes even when internal electrical filed is reduced. On the hand, if ratio at shorter wavelength will indicate any issue on p-layer or p-I interface. Fig 16 gives two QE ratio curves. One is from a good quality a-Si:H solar cell and the other is from a poor cell. We will review it later for different CA process a-SiGe:H and compare the quality of deposition films.

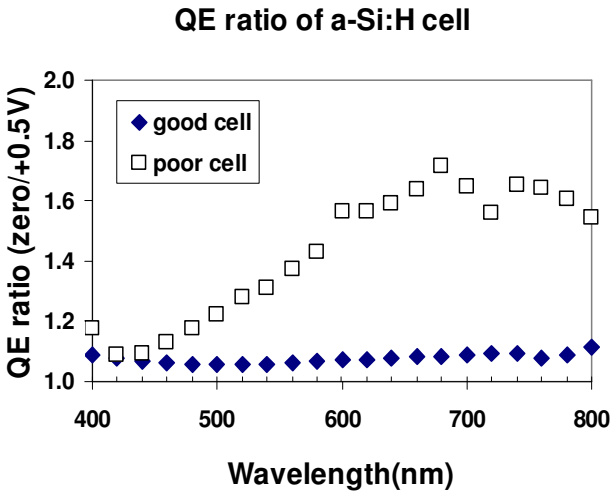

Figure 17 QE ratio of a-Si:H solar cells[1]

Hole μτ product

In a-SiGe:H solar, holes are normally minority carriers, except the region of p-i interface. This hole μτ product is fundamentally determine the quality of solar cell film

quality and also other performance of solar cell such as FF and QE. Large μτ product means that the holes can drift longer through each layer and with the assistant of the internal field and they can be collected. From QE equation, μτε product can be obtained by QE measurement. With known of thickness of intrinsic layer and absorption coefficient and electric field, the μτ product then can be derived.

Then how to calculate internal e-field become critical to hole μτ product. Dalal and Alvarez used a uniform electric field approximation by divided the sum of the applied and diffusion voltage by the thickness of intrinsic layer [35]. And then Crandall used a similar approximation to obtain the filed profile [36].

With above assumption, a constant electric field is applied and QE function is as below [35]:

$$QE(\lambda) = \frac{\alpha S_n}{1+\alpha S_n}[1-\exp(-\frac{t}{S_n}(1+\alpha S_n))]$$

where $S_n=\mu\tau\varepsilon$ is the range of holes.

According Dalal and Alvarez [35], we measure the quantum efficiency of the device for several wavelengths, as a function of applied voltage. If we assume that μτ doesn't change with small bias voltage and wavelength, the QE variation will be only comes from the change of the electric filed profile. At one wavelength, we can plot QE versus bias voltage. With the trial and error method, a suitable μτ can be used to make the measurement curve match the simulation curve, and this μτ product is the desired one. For best practice, long wavelength such as 600nm to 800nm is used. As for short wavelength, most of photons are absorbed near p-I interface, which cannot represent

intrinsic layer information. Figure 18 gives μτ product measurement result of one a-SiGe:H cell.

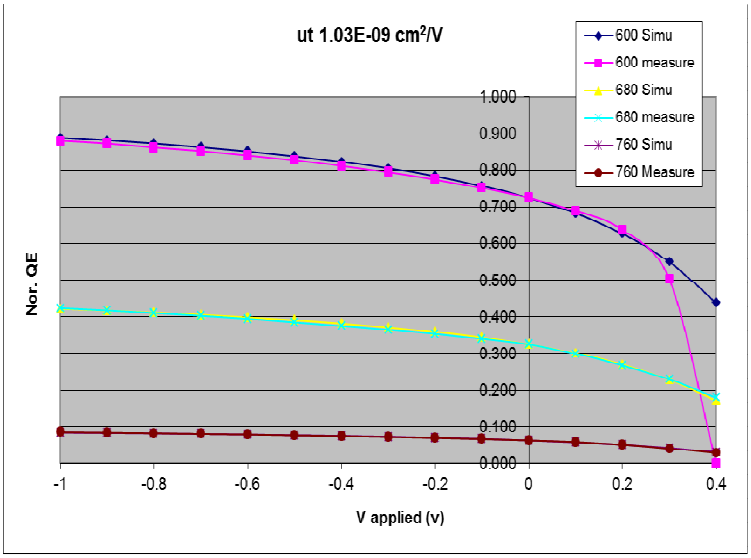

Figure 18 μτ measurement of a-SiGe:H solar cell

Urbach energy

The characterization of devices' Urbach energy follows the similar procedure described in QE measurement section. The only different between the QE measurement and Urbach energy measurement is that Urbach energy is measured in a long photon wavelength range, normally from 600nm to 1200nm for a-SiGe. The long wavelength is used to pick up information of tail state, as describe in early film Urbach energy section.

$$QE(\lambda) = \frac{\alpha S_n}{1+\alpha S_n}[1-\exp(-\frac{t}{S_n}(1+\alpha S_n))]$$

Above equation shows that QE is function with absorption coefficient. Then QE versus photon energy will be able to give the relationship between absorption

coefficients versus photon energy, which will be similar to Urbach energy measurement mentioned in film section. The Urbach energy from devices is obtained by the inverse slop of the natural logarithm of QE data versus photon energy, with help of the following equation.

$$\alpha = \alpha_0 \exp \frac{h\nu - E_g}{E_{ur}}$$

where E_g is the band-gap, h is Planck's constant and ν the wavelength

Figure 19 gives the Urbach energy measurement result of one a-SiGe:H solar cell based on the method mentioned above and the obtained value is 47meV.

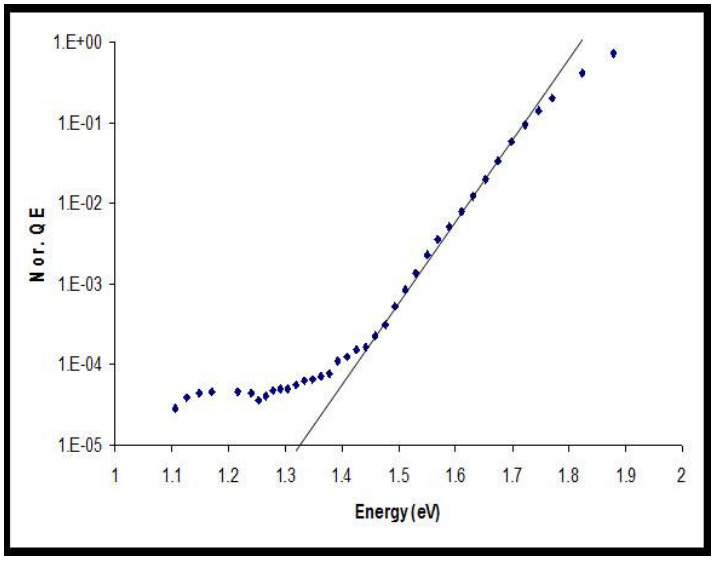

Figure 19 gives the Urbach energy measurement result of one a-SiGe:H solar cell

CHAPTER 4

Film Results

H2 CA FTIR results

As we discussed early, amorphous film exposed to H2 plasma becomes more ordered. Through H2 plasma exposure, abundant H- bond is reduced from film. In order to measure the effect of H2 plasma, we prepare deposit amorphous SiGe:H film on glass substrate (for FTIR double polish Si wafer was used as mentioned in early chapter) and film thickness is carefully controlled around 1um. It will help to precisely normalize H2 concentration. During the deposition, H2 plasma exposure time is automatically controlled. While H2 follow is constant during the whole deposition time, SiH4 and GeH4 are turned off during H2 annealing time, as chart showed in below

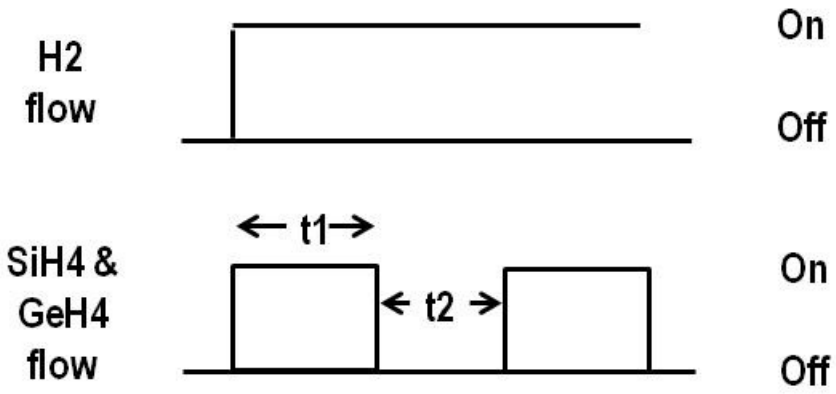

Figure 20 Gas flow configuration during chemical annealing process

Deposition time t1 is constant at 10 second, while H2 annealing time varied from 10 sec to 30sec. Below charts show the normalized comparison among different annealing time.

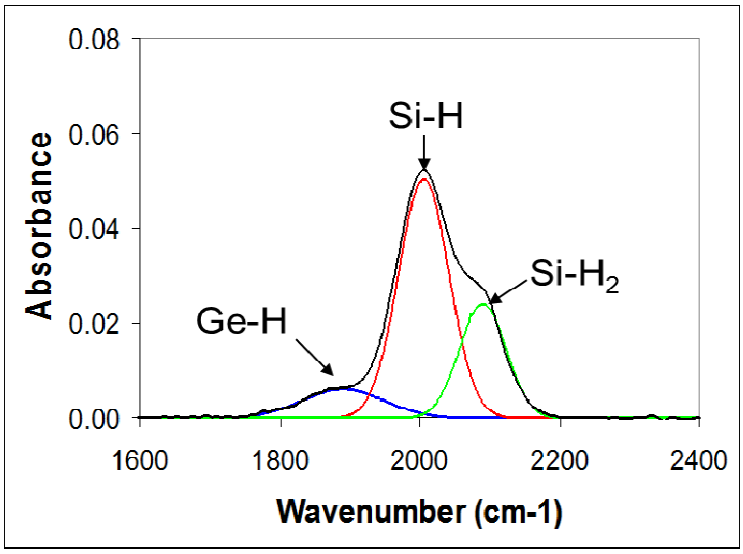

Figure 21 Non-CA sample FTIR

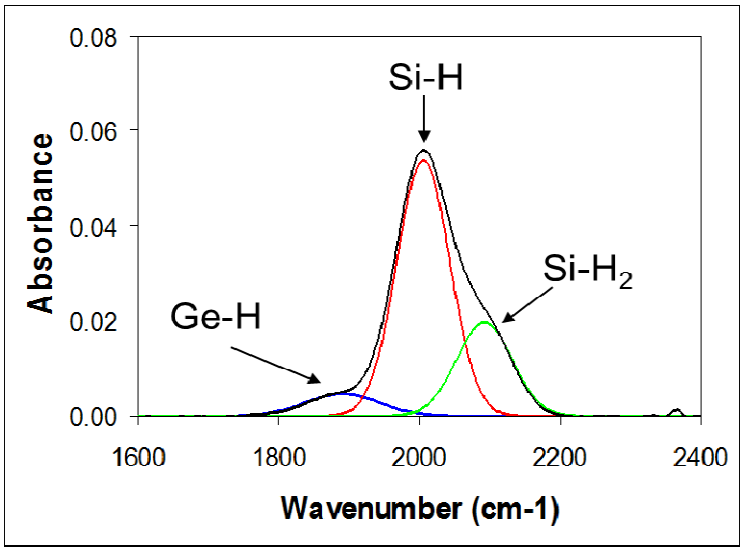

Figure 22 10 second H2 CA sample FTIR

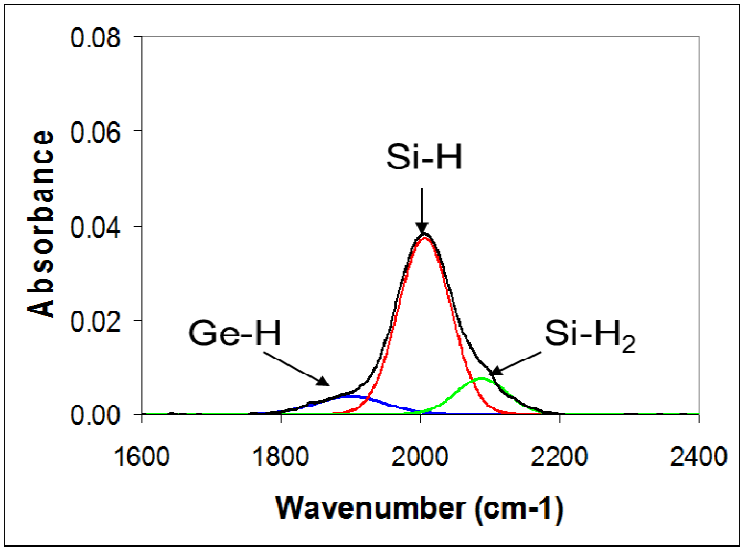

Figure 23 20 second H2 CA sample FTIR

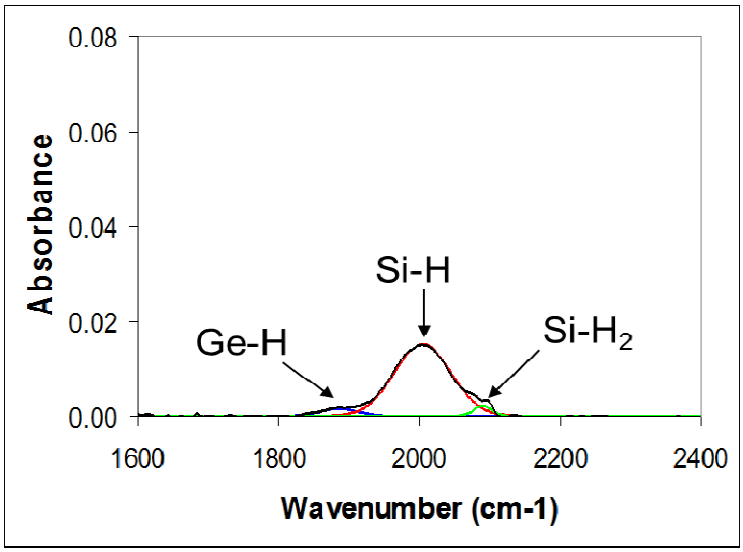

Figure 24 30 second H2 CA sample

Above figures show the FTIR data for samples with same deposition time but different hydrogen CA times. We found that with help of H2 chemical annealing, abundant H- bond could be significantly altered. Meanwhile, no significant Ge-H2 bond

was noticed in FTIR test. However, the film quality is more depends on the ratio of Si-H to Si-H2 bond.

The following graph shows the hydrogen content and Si-H to Si-H2 ratio calculated from FTIR data.

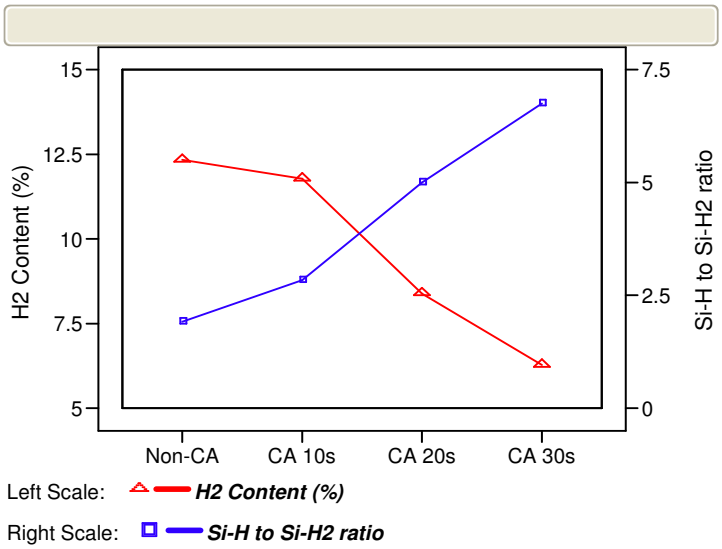

Figure 25 H2 concentration & Si-H to Si-H2 bond ratio

Above charts shows through H2 chemical annealing process, Si-H2 contents were reduced. The ratio of Si-H to Si-H2 bond intensity is 7 for 30 sec CA film and 2 for non- CA film. And CA help to reduce H content from 12% (non-CA) to 6% (30s H2 CA), which is calculated from H- related bond. On the contrary from previous Si CA works, the a-SiGe:H remains amorphous phase all the time even with 30sec CA time, based upon Raman results.

Film FTIR shows that CA helps to improve the microstructure but reduce the Si-H to Si-H2 ratio. Meanwhile H2 content was reduced as well which limit the light soaking degradation, which we will discussed in later device section.

Electrical data

The films are deposited on stainless steel substrate and same CA deposition method was described as above. Then we measure the photo conductivity as below:

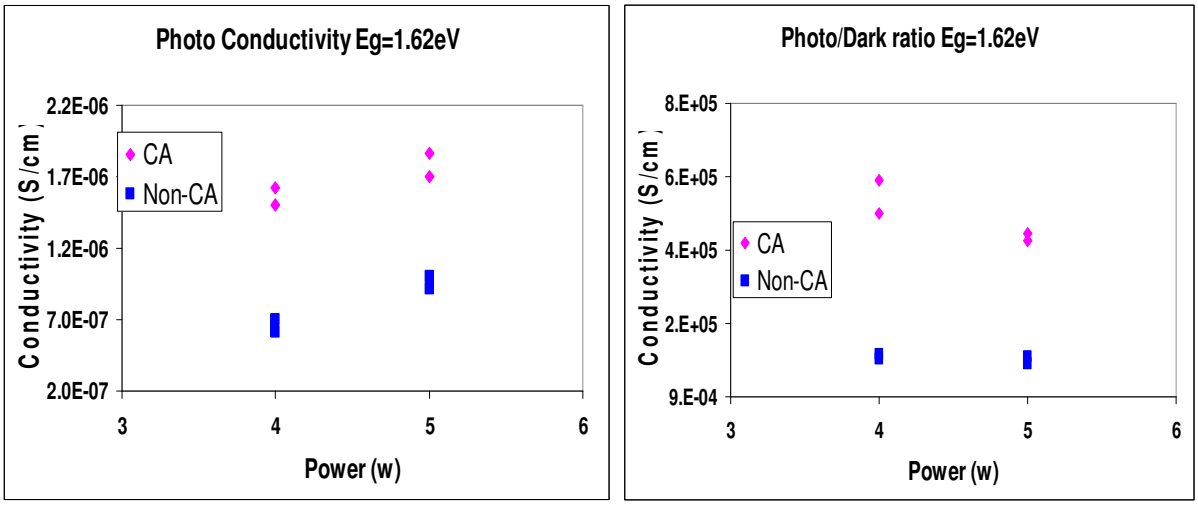

Figure 26 Photo Conductivity and Photo/Dark ratio

Above picture shows the compare between CA anneal samples vs. non-CA samples. It was found that CA films give better microstructures and CA films show better photoconductivity and higher photo/dark ratio. Meanwhile Urbach Energy of CA films is in the range of 45~50meV. Based upon films, the electron mobility-lifetime product were measured,

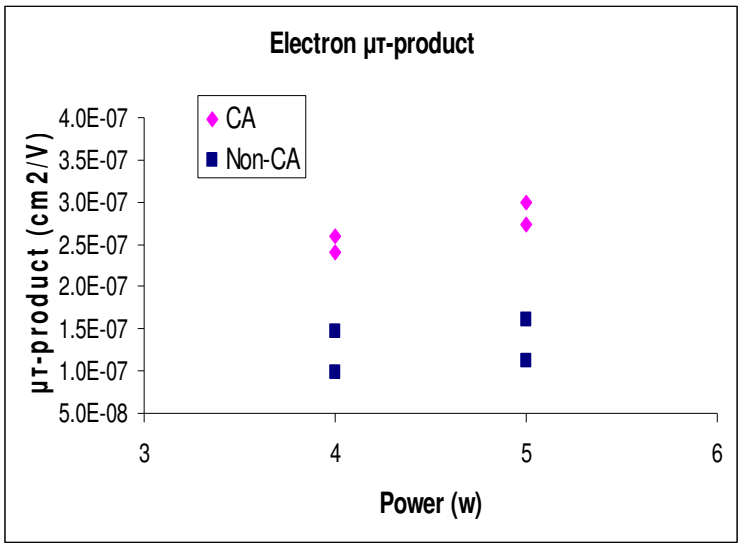

Figure 27 μτ -product of a-SiGe:H film at Eg=1.62eV

It is clear that CA films have higher electron mobility-lifetime product. With CA method, better quality a-SiGe:H film could be achieved. Above results shows in most of aspects, CA film shows better or equal quality compared to non-CA film.

Chapter 5

Devices results

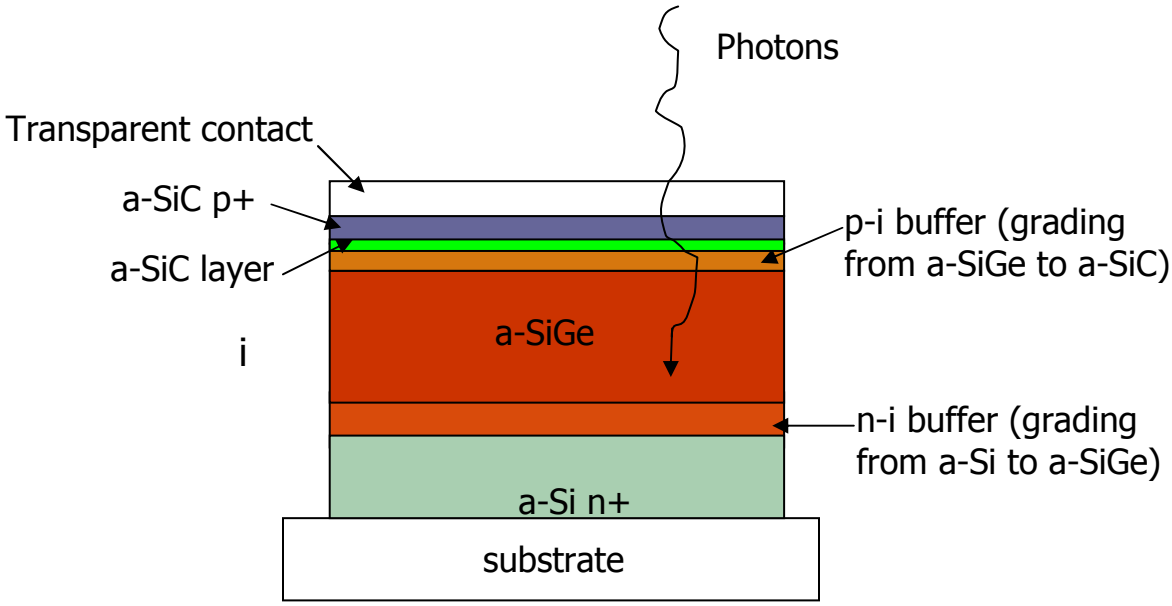

Figure 28 Typical a-SiGe:H solar cell device structure

Above pictures shows a simples device structure we used. It is simple structure with ITO/p+in+ on stainless steel substrate. Meanwhile, this structure has no back reflector and no light trapping.

I-V Curves

In order to compare the effect of CA in device level, samples are prepared in the same way except the intrinsic layer. Non-CA samples are using normal deposition method, CA samples use 10s CA method as standard method.

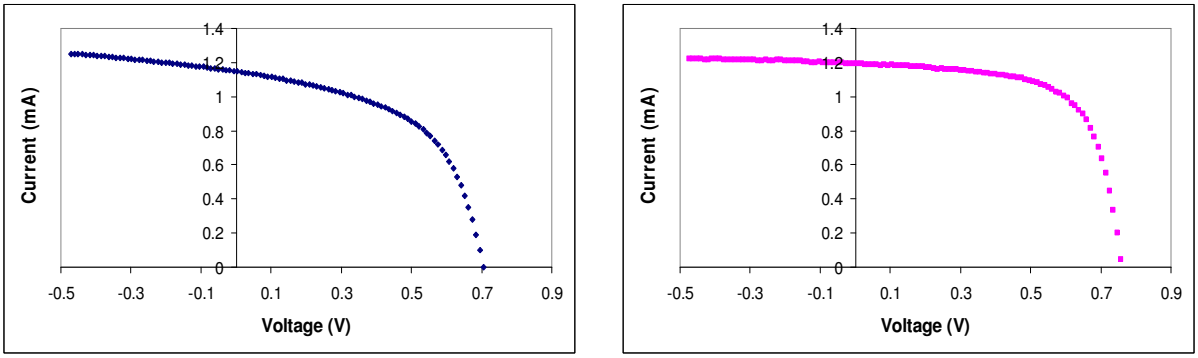

Non-CA CA samples

Figure 29 IV-curve comparisons between non-CA and CA samples

Above figures shows the compare between Non-CA devices with CA devices. It was found that CA device has slightly higher Voc and Isc than Non-CA samples. And by CA approach, better fill factor device (65.5%) was achieved, as below under condition of 100mT and 300C substrate temperature. (Voc=0.7901V, Isc= 1.442mA, FF=65.5 w/ Al bar)

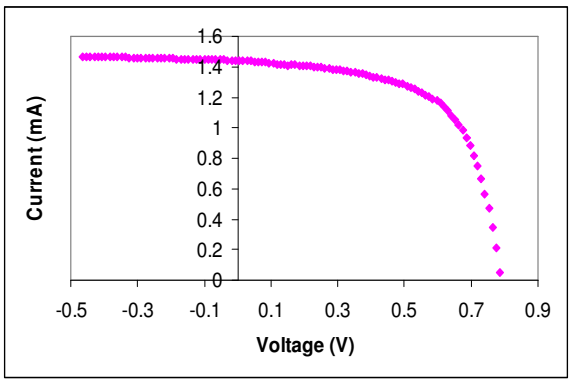

Figure 30 IV-curve of a-SiGe:H sample with 65.5 FF

Quantum Efficiency

Another critical factor of device performance is the quantum efficiency at reduced electrical field. Thus, we collected the QE from above two samples under 0V and positive bias.

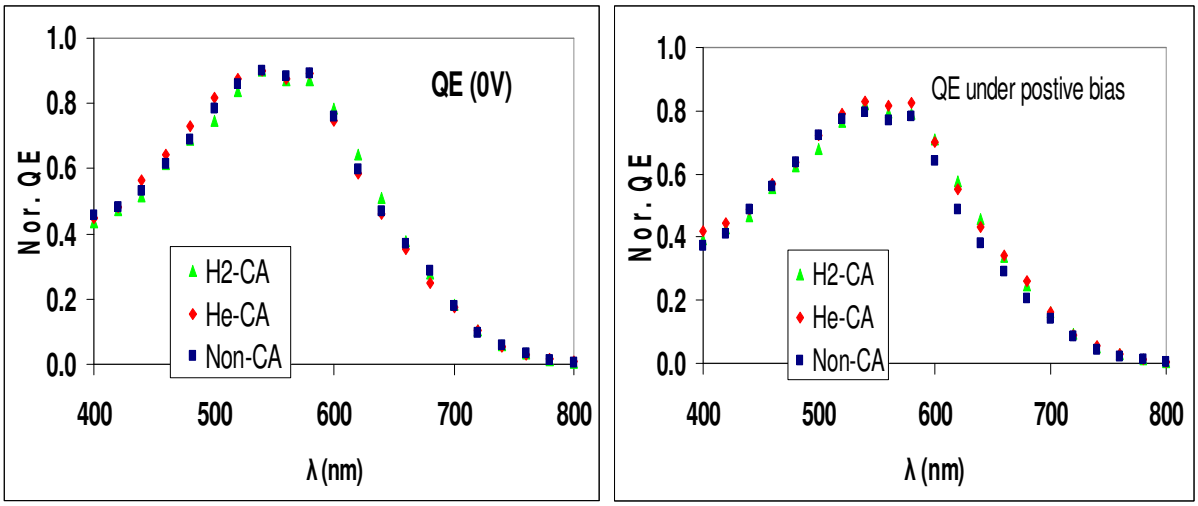

Figure 31 QE comparisons between different samples under zero bias and positive bias

Above figures shows the comparison among Non-CA devices, H2 CA devices and He CA devices. QE under 0 bias overlapped. However QE under positive bias from Non-CA suffer at long wavelength.

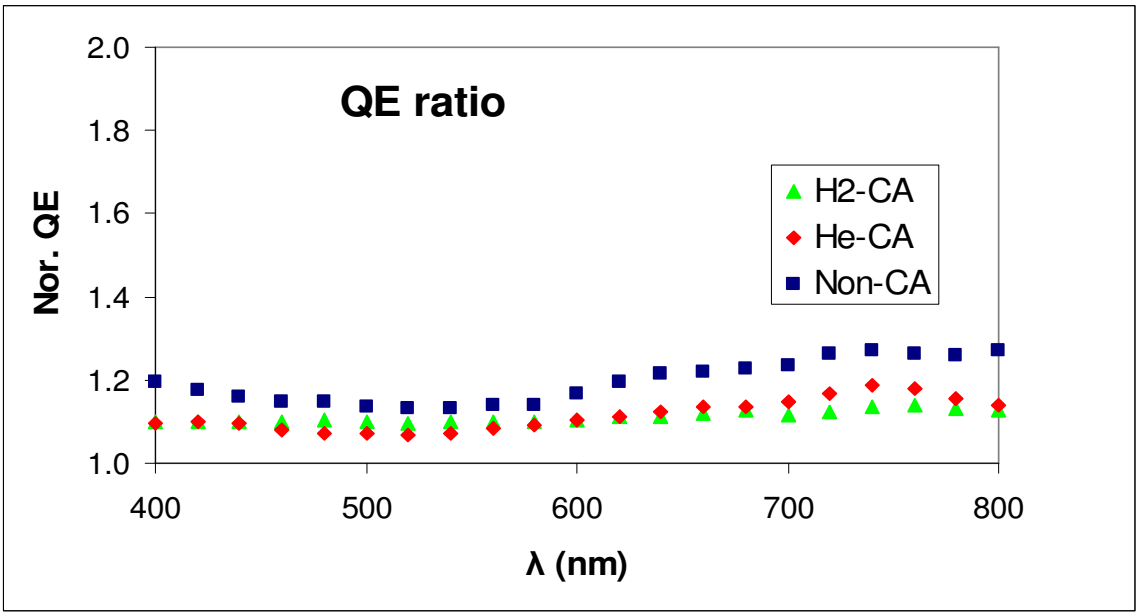

Figure 32 QE ratio comparisons among Non-CA, H2-CA, He-CA samples

The QE ratio experiment reveals the influences of a decreased electric field on the carrier collection. It is found that smaller change in long wavelength QE ratio for the annealed cells. This indicates that holes are being collected relatively efficiently. It could explain why better FF was achieved by using CA method

Hole Mobility-lifetime product

Systemic study on hole mobility-lifetime product was done to compare the CA effect on devices. We studied the CA samples prepared under different pressure condition, as we know during CA time, H ion bombardment varied with pressure.

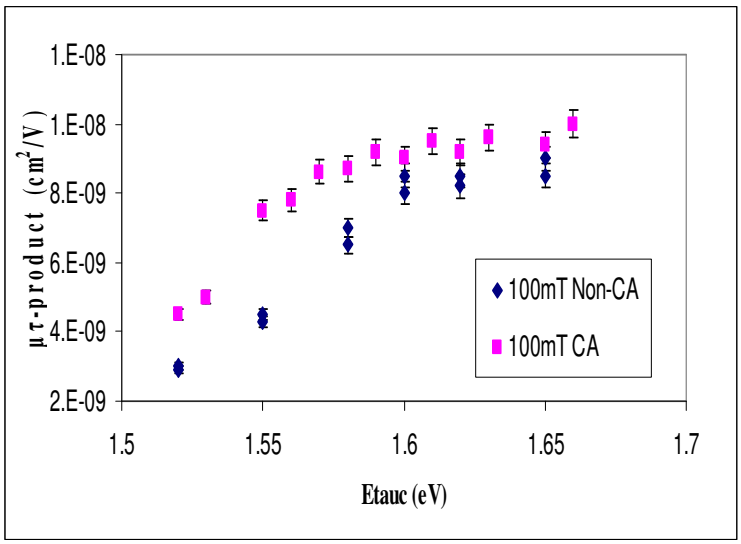

Figure 33 100mT μτ -product comparisons between H2-CA and Non-CA samples

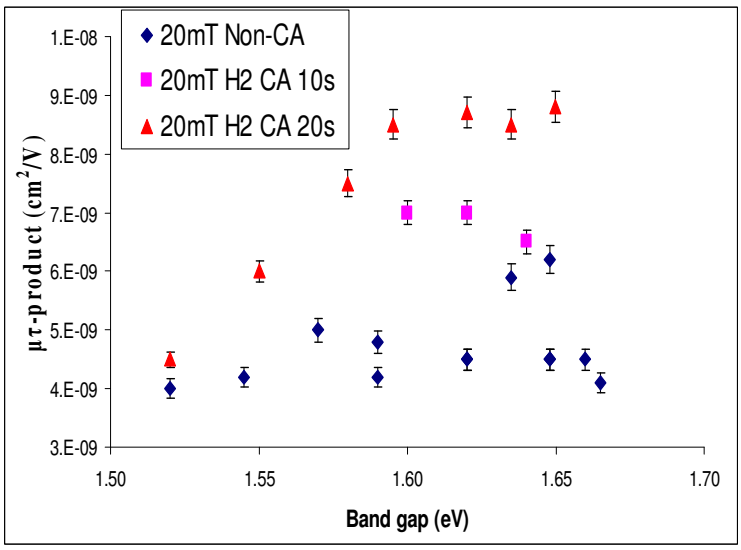

Figure 34 20mT μτ-product comparisons among H2-CA 10sec, H2-CA 20sec and non-CA samples

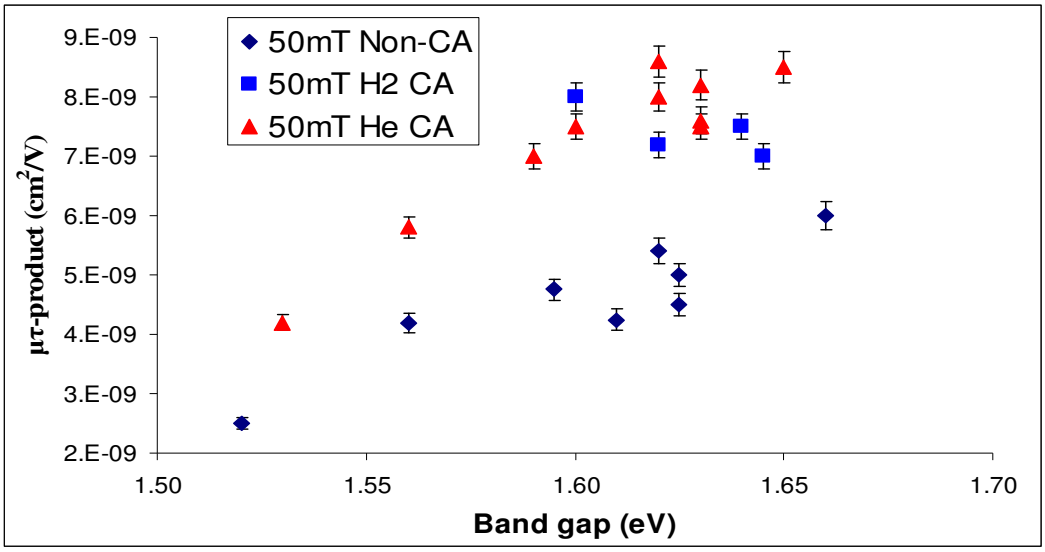

Figure 35 50mT μτ-product comparisons among H2-CA, He-CA and Non-CA samples

Above figures show that among all above pressure conditions, 20mT, 50mT & 100mT, CA samples have higher hole μτ and H2 CA devices achieve better hole μτ at 20s annealing time. We could find that hydrogen and helium could help us improve the quality of a-SiGe materials, which lead to better a-SiGe solar cell application.

Light soaking

Another benefit of CA prepared samples, are significantly improve the lifetime of solar cells. In order to demonstrate lifetime of solar cell itself, we use 2x sun exposure to accelerate the degradation of cells.

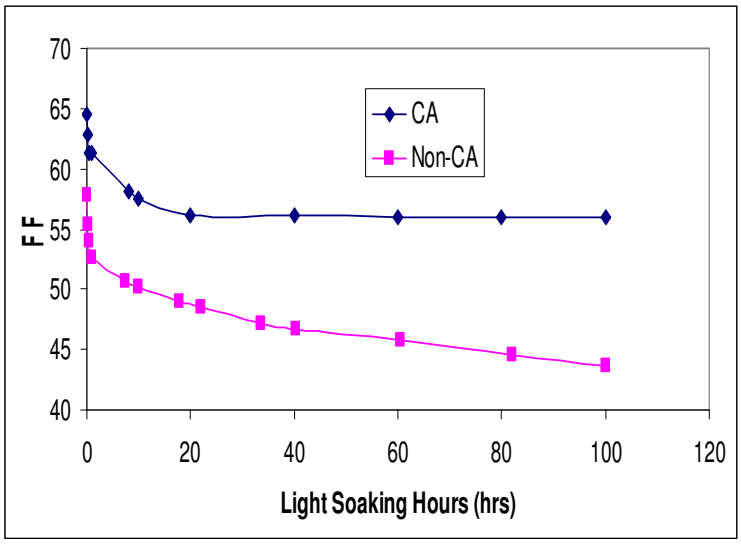

Figure 36 FF degradation of CA and Non-CA samples

We monitors the FF of CA (10s H2) and non-CA samples while exposed them to 2x sun light at same time. The results show that non-CA samples degrade much faster than CA samples. And after 20 hour light soaking, CA sample FF stop further degradation and FF remains at 57%. On the other hand, non-CA sample continue degrading even after 100 hr light soaking, which is consistent with a-SiGe:H performance in literature.

Another aspect to understand the cell degradation is by checking QE the solar cell before and after light soaking test.

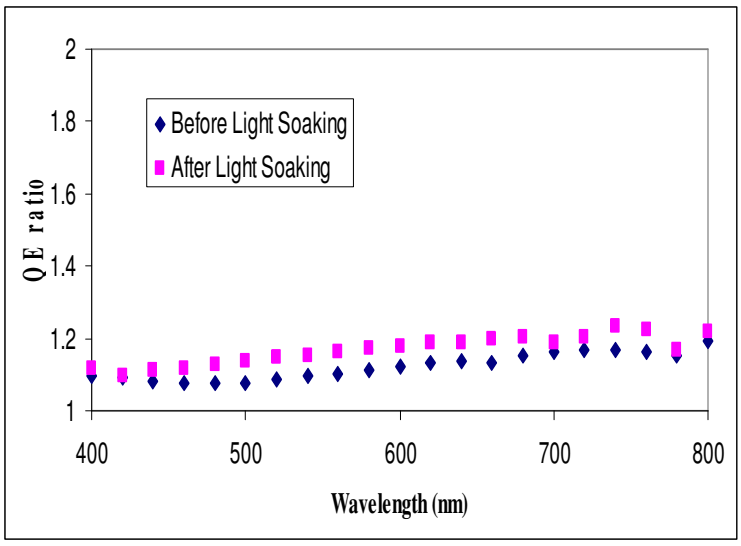

Figure 37 QE ratio before and after light soaking of CA samples (10s H2)

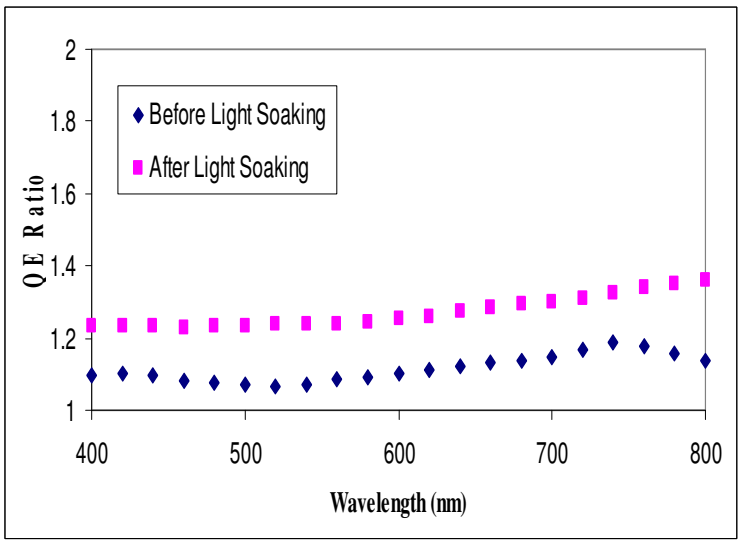

Figure 38 QE ratios before and after light soaking of non-CA samples

Above two charts shows the non-CA sample and CA samples QE performance before and after light soaking. Non-CA sample shows strong degradation of QE, which means cell's capability of collection carriers, is significantly degrade after light soaking. On the contradictory, CA sample (10s H2) did not show very strong degradation. Minor

difference is noticed, which is aligned with FF reduction after 20 hrs light soaking. However, overall performance is much better than non-CA sample, which is constant with more stable and better FF than non-CA samples shown in early chart.

CHAPTER 6

CONCLUSIONS

In summary, a preliminary and careful study has been carried out of the growth and properties of a-SiGe:H films and devices based on chemical annealing and non chemical annealing techniques. The films and devices were grown using VHF-plasma at ~45Mhz. The following significant results were obtained:

- Chemical annealing using hydrogen or helium leads to improvements in hydrogen microstructure.
- CA is a promising technique to improve the quality of a-SiGe materials for solar cell applications.
- The ratio of Si-H to Si-H2 bond increased significantly. With the assistant of CA, H content in SiGe could be reduced
- CA films show better photoconductivity and higher photo/dark ratio
- CA films have higher electron mobility-lifetime product
- Smaller change in long wavelength QE ratio for the annealed cells. This indicates that holes are being collected relatively efficiently.
- Systemic study on one deposition time but with different CA time,10s, 20s… at different CA pressure show hole mobility lifetime was improved through CA process.
- With improvement in many aspects, CA devices have better FF (65.5%).
- Light soaking results show CA devices has longer lifetime and more stable than non-CA devices.

REFERENCES

[1] Nanlin Wang, Improving the stability of amorphous silicon solar cells by chemical annealing 2006

[2] K.Tanaka, E.Maruyama, et al., Amorphous Silicon, John Wiley & Sons, New York, 1998.

[3] D.L. Staebler and C.R. Wronski, Appl. Phys. Lett., 31 (1977) 292

[4] Donald A. Neamen, "Semiconductor Physics and Devices", 3rd edition, McGraw-Hill, New Delhi, 2003.

[5] J.H. Moller, Semiconductors for Solar Cells, Artech Hous Inc., MA (1993)

[6] W. Luft and Y. Tsuo, Hydrogenated Amorphous Silicon Alloy Deposition Processes, Marcel Dekker, Inc., New York (1993)

[7] D. Adler, Semiconductors and Semimetals, 21 Academic Press, New York, (1984)

[8] V.L. Dalal et al., Mat. Res. Soc. Symp. Proc. 149 (1989) 601

[9] H. M. Branz, Phys. Rev. B, 59 (8), (1999) 5498

[10] Sukti Hazra et al. India Association for the Cultivation of Sci. Rf-plasma enhanced CVD

[11] S. Shimizu, H. Miyahara et al., J. of Non-Crystalline Solids, 338-340 (2004) 47

[12] S. Shimizu, M. Kondo, and A. Matsuda, J. Appl. Phys., 97 (2005) 033522

[13] V.L. Dalal, Thin Solid Films, 395 (2001) 173

[14] A.H Mahan, D.L. Williamson, B.P. Nelson, and R.S. Crandall, Physical Review B, 40 (1989) 12024

[15] V.L. Dalal, G. Baldwin et al., AIP Conference Proceedings, 306 (1994) 460

[16] W. Futako, T. Kamiy, I. Shimizu, J. of Non-Crystalline Solids, 266-269 (2000) 630

[17] K. Ohkawa, S. Shimizu et al., Solar Energy Materials & Solar Cells, 66 (2001) 297

[18] W. Futako, and I. Shimizu et al., J. of Non-Crystalline Solids, 198-200 (1996) 1046

[19] S. Miyazaki, N. Fukuhara and M. Hirose, J. Non-Cryst. Solids, 266 (2000), 59

[20] H. Sato, K. Fukutani et al., Solar Energy Materials & Solar Cells, 66 (2001) 321

[21] Yong Liu, High growth rate deposition of hydrogenated a-SiGe films and devices using ECR-PECVD (ISU, dissertation, 1995) 17.

[22] A. Matsuda, M. Koyama, N. Ikushi et al., Japn. J. Appl. Phys. 25 (1986) 54

[23] J. Perrin, M. Shiratani, K. Patrick et al., J. Vac. Sci. Technol. A 16(1) (1998) 278

[24] A. Gallagher, J. Appl. Phys., 63(7) (1988) 2406

[25] V.L. Dalal, R. Knox et al., Conference Record of the IEEE Photovoltaic Specialists Conference, 22nd(2) (1991)1399.

[26] V.L. Dalal, T. Maxson et al., J. of Non-Crystalline Solids, 227-230 (1998) 1257.

[27]S.K. Kaushal, Growth of high Quality a-(Si,Ge):H films using low pressure, remote ECR plasma technique 17, (ISU, thesis, 1995)

[28] D.K. Schroder, Semiconductor Material and Device Characterization, John Wiley & Sons, Inc. New York, 1998.

[29] M. Bermejo, M. Cardona, J. Non-Cryst. Solids, 32 (1979) 413

[30] B.W. Faughnan and R. Crandall, Appl. Phys.Lett., 44 (1984) 537

[31] M.H. Brodsky, M. Cardona, and J.J. Cuomo, Phys. Rev. B, 16 (1977) 3556

[32] C.J. Fang, K.J. Gruntz, L.Ley, et al. J. Non-Cryst. Solids. 35&36 (1980) 255

[33] S. Lee, S. Kumar, and C. Wronski, J. Non-Cryst. Solids 114, (1989) 316

[34] S. M. Sze, Physics of Semiconductor Device, 2nd Edition, John Wiley & Sons, Inc. New York, (1998)

[35] V.L. Dalal, and F. Alvarez, Journal De Physique, Supplement C4, 42 (1981) 491

[36] D.E. Crandall, and C.R. Wronski, Applied Physics Letters, 28 (11) (1976) 671